

# H I 21 cm Extended Structures to the North-East, and South-West of NGC 5595: VLA Observations of the Disk Galaxy Pair NGC 5595 and NGC 5597

J. ANTONIO GARCIA-BARRETO<sup>1</sup> AND EMMANUEL MOMJIAN<sup>2</sup>

<sup>1</sup>*Instituto de Astronomia, Universidad Nacional Autónoma de México,  
Apartado Postal 70-264, Ciudad de México 04150, México*

<sup>2</sup>*National Radio Astronomy Observatory, P. V. D. Science Operations Center,  
P.O. Box O, Lovelock Road, Socorro, 87801-0387, New Mexico, U.S.A.*

(Accepted March 31, 2023)

## ABSTRACT

We report VLA B-configuration observations of the H I 21 cm line on the close disk galaxy pair NGC 5595 and NGC 5597. At the angular resolution of the observations,  $\sim 7''.1 \times 4''.2$ , while most of the H I 21 cm in NGC 5595 and in NGC 5597 has the same extent as the optical disk, we have detected for the first time extended structures (streamers) to the north-east (NE), and south-west (SW) of NGC 5595 with no counterparts in blue, red optical (continuum), 20 cm radio continuum, or H $\alpha$  spectral-line emission. One structure is extended by  $\sim 45''$  to the NE with blue-shifted velocities, and the other by  $\sim 20''$  to the SW with red-shifted velocities with respect to the systemic velocity. No H I 21 cm emission is detected from the innermost central (nuclear) regions of either galaxy. Lower angular resolution H I 21 cm imaging indicates the non-existence of any intergalactic H I 21 cm gas as tails or bridges between the two galaxies. Our new 20 cm radio continuum emission image of NGC 5597 shows a strong unresolved elongated structure at the central region, in the north-east south-west direction, very similar to the spatial location of the innermost H $\alpha$  spectral line emission. There is no 20 cm continuum emission from its north spiral arm. In NGC 5595, the 20 cm radio continuum image shows no continuum emission from the NE nor the SW extended structures with H I 21 cm emission.

*Keywords:* galaxies: active: individual (NGC 5595, NGC 5597) —galaxies: kinematics and dynamics  
— galaxies: ISM — galaxies: spiral

## 1. INTRODUCTION

From the observational point of view, ongoing major and minor gravitational interactions of two or more disk galaxies show extended H I 21 cm cold gas structures of tidal origin, with M51 and NGC 5195 being one of the classic examples (Sancisi 1999).

The numerical simulations performed by citettoo72 have convincingly shown that the gravitational interactions in very close pair of disk galaxies in their late stages of merging cause stellar tails and bridges (e.g., M51 with NGC 5195, NGC 4038 with NGC 4039, NGC 4676A with NGC 4676B – the mice). They went even further and dared to raise the possibility that the in-

nermost density-wave spiral pattern in galaxies such as M51 and NGC 7753 was caused indirectly by the recent external influences (see their section VII subsection *d*) ending with the question, *Et tu M81?* referring to M81 with the close companion NGC 3077).

Since then gravitational interaction between a close pair of disk galaxies has been recognized to be important in determining their gas kinematics, dynamics, star formation, central feeding of a massive black hole and their evolution in time (Mihos & Hernquist 1994, 1996).

Recent galaxy distribution surveys have confirmed that galaxies are found in a hierarchical structure of filaments and walls that surround large galaxy voids with 54% in the local universe concentrated in virialized clusters and groups, and only 7% as isolated pairs of galaxies (Argudo-Fernandez et al. 2015). Galaxy pairs detected in the far infrared by the Infrared Astronomical

Satellite (IRAS) have a median separation of  $20 h^{-1}$  kpc, and pairs that are most probably close together in space have greater specific star formation rates (SSFR) (Geller et al. 2006). Using H $\alpha$  line emission to estimate star formation rate in major mergers<sup>1</sup> from 2409 galaxies reveals enhanced star formation in cases where the gravitational tidal force is relatively strong compared to the self-gravity of a galaxy (Woods & Geller 2007). These authors also found that for major mergers there is a correlation between SSFR and separation (on the plane of the sky),  $\Delta D$ , in such a way that the smaller  $\Delta D$  the higher the SSFR (Woods & Geller 2007).

Radio continuum observations at  $\lambda \sim 11$  cm,  $\lambda \sim 6$  cm and  $\lambda \sim 3.7$  cm of disk-disk pairs from the Catalog of Isolated Pairs of Galaxies (CPG; Karachentsev 1972) revealed a correlation between physical separation and radio emission, with close pairs being radio emitting sources at more than twice the number than more widely spaced pairs (Stoche 1978; Stoche et al. 1978). Westerbork radio interferometer continuum observations at 1.415 GHz have shown that the radio power of the central sources in pair of galaxies is on average four times higher than in isolated disk galaxies (Hummel 1981; Hummel et al. 1987). Furthermore, Very Large Array radio continuum observation at 1.46 GHz and 4.88 GHz of 60 *interacting* galaxies have shown that on average the radio power of the central radio sources are about a factor of five higher than in isolated galaxies, and that the radio power of central radio sources in barred disk galaxies are a factor of five higher than in non-barred disk galaxies (Hummel et al. 1987, 1990).

What Toomre & Toomre (1972) did not explicitly state was that narrow and long tails and bridges of cold H I 21 cm gas are also caused by gravitational interaction of close pairs of disk galaxies. Indeed, three of the most beautiful examples of H I 21 cm imaging of interactions in a system of galaxies are: i) NGC 5194 (M51, Sbc(s)I-II) with its SE long tail and its companion NGC 5195 (SB01 pec) (Davies 1974; Haynes et al. 1978; Appleton et al 1986; Rots, et al. 1990), ii) the M81 (Sb(r)I -II) – M82 (amorphous) and NGC 3077 (Irr) system with cold atomic hydrogen gas structures from a northern tidal bridge between M82 and NGC 3077, a southern tidal bridge between NGC 3077 and M81, and the structure between M81 and M82 (Cottrell 1976; van der Hulst 1979; Yun, Ho & Lo

1993, 1994), and iii) NGC 4038/4039 “the antennae”, NGC 4038 SB,(s)mpec NGC 4039 SAB(s)mpec (van der Hulst 1979; Gordon, Koribalski & Jones 2001; Hibbard et al. 2001).

One such nearby disk galaxy pair system is NGC 5595 and NGC 5597. For this system, we adopt a Hubble (spectroscopic) distance of  $D_{\text{pair}} = 38.6$  Mpc (Tully 1988), giving an approximate angular-to-linear scale of  $1'' \sim 187.14$  pc. The projected separation (on the plane of the sky) between the two galaxies is  $\sim 3'.97$ , or  $\sim 45$  kpc. Our analysis of the H I 21 cm gas emission, rotation curve, and angular velocity in NGC 5597 using data obtained with the Karl G. Jansky Very Large Array (VLA)<sup>2</sup> in B-configuration, and the subsequent estimation of the angular velocity pattern of its stellar bar have already been reported (Garcia-Barreto & Momjian 2022).

Since NGC 5595 and NGC 5597 are so close on the plane of the sky, it required a single VLA pointing (primary beam full width at half power,  $\theta_{\text{HPBW}} = 30'$  at 1.4 GHz) to observe the H I 21 cm emission from the disk galaxy pair system. Therefore, here we report the overall H I 21 cm kinematics and dynamics of each disk galaxy and their close environment.

NGC 5597 was originally chosen from a list of 56 nearby, bright, barred galaxies with IRAS  $60\mu\text{m}$  flux densities greater than 5 Jy (Garcia-Barreto et al. 1996) and colors indicative of circumnuclear star formation (Helou et al. 1985). Its IRAS flux densities are  $f_{60\mu\text{m}} \sim 8.7$  Jy,  $f_{100\mu\text{m}} \sim 15.32$  Jy with  $T_{\text{dust}} \sim 36^\circ$  K. In 1996, we were only aware that NGC 5597 was part of Tully’s group 41+15+15. Later, we carried out the study of companions for the same set of nearby bright barred galaxies utilizing NED<sup>3</sup> database and found out that NGC 5597 has only one nearby disk galaxy companion, namely NGC 5595 (Garcia-Barreto, Carrillo, & Villamizar 2003). Based on their projected spatial proximity ( $\Delta D_{12}/(d_1+d_2) \leq 2$  (Zwicky 1956; Karachentsev 1972, 1981)) and very similar spectroscopic H I 21 cm systemic velocities ( $\Delta V \leq 5$  km s<sup>-1</sup>), NGC 5597 forms an isolated gravitationally bound pair with the disk galaxy NGC 5595 (Sc).

There is also growing evidence of weak nuclear activity in normal disk galaxies with and without a prominent stellar bar, with observational detection of nuclear

<sup>1</sup> Major mergers have been defined as pair of galaxies whose difference in apparent magnitude is less than 2,  $\Delta m \leq 2$ ; minor mergers on the contrary are pair of galaxies whose difference in apparent magnitude is more than 2,  $\Delta m \geq 2$  (Woods & Geller 2007).

<sup>2</sup> The National Radio Astronomy Observatory is a facility of the National Science Foundation operated under cooperative agreement by Associated Universities, Inc.

<sup>3</sup> The NASA/IPAC Extragalactic Database (NED) is operated by the Jet Propulsion Laboratory, California Institute of Technology, under contract with the National Aeronautics and Space Administration.

low velocity bipolar outflows in H $\alpha$ , e.g., M81 (Goad 1976), NGC 1068 (Ulvestad, Neff & Wilson 1987), M51 (Ford et al. 1985; Cecil 1988; Crane & van der Hulst 1992; Scoville et al. 1998), NGC 3079 (Veilleux et al. 1994), M101 (Moody et al. 1995), NGC 3367 (Garcia-Barreto et al. 1998, 2002), and NGC 1415 (Garcia-Barreto et al. 2019), suggesting that they represent a low end of scale for nuclear activity after quasars, BL Lac objects, radio galaxies, and Seyfert galaxies. All such phenomena have an origin in events occurring around central massive black holes with the level of the activity being governed by the gas supply to fuel these central engines (Norman & Silk 1983). Similar physical processes have also been observed in NGC 3367 (Garcia-Barreto et al. 1998, 2002, 2005; Hernández-Toledo et al. 2011).

In this paper, we present VLA B-configuration observations of atomic hydrogen, HI 21 cm, cold gas emission at an angular resolution of  $7''.1 \times 4''.2$  at P.A.  $\sim -10^\circ$  EofN (or about  $1.33 \times 0.78$  kpc in linear size), as well as new 20 cm radio continuum emission from the disk galaxy pair NGC 5595 and NGC 5597. We have imaged the global HI 21 cm emission from this galaxy pair to probe the internal kinematics, and investigate the existence of any large scale gas structure between them. We have also made 20 cm radio continuum emission images for both disk galaxies. For the barred galaxy NGC 5597, we compare its 20 cm continuum emission with previously published H $\alpha$  spectral line emission and blue optical (broad band continuum from 103aO glass plate)

spatial distribution, especially in the inner  $30''.0$ . This work is organized as follow: § 2 presents the observations and data reduction. § 3 presents the disk galaxy system as an isolated gravitationally bound pair. § 4 presents some properties of NGC 5597 as an SBc disk galaxy. § 5 presents some properties of NGC 5595 as an Sc disk galaxy, § 6 presents the HI 21 cm features in the field of the disk galaxy pair NGC 5595 and NGC 5597, and finally § 7 presents the summary and conclusions.

## 2. OBSERVATIONS AND DATA REDUCTION

Two dimensional velocity fields for the HI 21 cm emission from the disk galaxy pair NGC 5595 and NGC 5597 were obtained using the VLA in its B configuration on 2019 June 6, 7, 11, 16, 18, & 22. In each day, the total observing time was about  $1.5^h$  and included 100 min of on-source time, as well as overhead to observe the flux density scale calibrator/bandpass calibrator 3C 286, and the complex gain calibration J1448–1620. The VLA system was tuned to the rest frequency of the HI 21 cm line  $\nu_{\text{rest}} = 1,420,405.752$  kHz redshifted to a mean heliocentric velocity of  $v_{\text{pair}} = 2,700$  km s $^{-1}$  for the galaxy pair system. Table 1 lists the coordinates, Hubble type, distance, and systemic HI velocities of the two galaxies NGC 5595 and NGC 5597. Furthermore, because these two galaxies are separated by only  $\leq 4'$  on the plane of the sky, and are well within the primary beam of the VLA antennas ( $\theta_{\text{HPBW}} = 30'$  at 1.4 GHz), the pointing center of the observations was chosen to be midway between the two disk galaxies:  $\alpha_{\text{mid}} = 14^h 24^m 21.^s0$ ,  $\delta_{\text{mid}} = -16^\circ 44' 45''.0$ .

**Table 1.** NGC 5595 - NGC 5597 Pair of Disk Galaxies: Coordinates, Hubble type, Distance, Systemic HI Velocity

Galaxy Name	$\alpha(\text{J2000})$ <i>hh mm ss</i>	$\delta(\text{J2000})$ $^\circ \ ' \ ''$	Ref.	RSA type	NED type	Distance Mpc	Ref.	$V(\text{HI})_{\text{sys}}$ km s $^{-1}$	Ref.
(1)	(2)	(3)	(4)	(5)	(6)	(7)	(8)	(9)	(10)
NGC 5595	14 24 13.3	−16 43 21.6	1	Sc(s) II	SAB(rs)c	38.6	2	2697	3
NGC 5597	14 24 27.49	−16 45 45.9	1	SBc(s) II	SAB(rs)b	38.6	2	2698	3

NOTE—1) (Diaz-Hernández et al. 2009), 2) (Tully 1988), 3) (Paturel et al. 2003)

The observations utilized one of the 1 GHz wide 8-bit sampler pairs of the VLA, namely A0/C0, and the Wideband Interferometric Digital ARchitecture (WIDAR) correlator was configured to deliver a single 4 MHz wide

subband with 256 spectral channels, resulting in a channel spacing of 15.625 kHz or 3.3 km s $^{-1}$ . This subband spans a velocity range of  $\Delta V \sim 843$  km s $^{-1}$ , which is sufficient to cover the full width at zero intensity of the HI emission from both NGC 5595 and NGC 5597, and provide line-free channels for continuum subtraction.

We used the Common Astronomy Software Applications (CASA) for the flux density scale, bandpass, complex gain calibration, continuum subtraction, as well as deconvolution and imaging. The Astronomical Image Processing System (AIPS) was utilized for the spectral and kinematics analysis, and for the presentation and overlay of 20 cm continuum, H $\alpha$  and optical 103aO images.

The data set of each session was calibrated independently, and image cubes were made to determine the line-free channels for continuum subtraction. Line+continuum emission from NGC 5597 was confined between channels 81 to 200, and from NGC 5595 between channels 81 and 197. The continuum emission was subtracted from the line+continuum data in the  $uv$  plane. The H I image cube was then produced by combining the data from all the sessions, using a cell size of 1''0 and Briggs weighting with robust=0.8. The resulting synthesized beam was  $\sim 7''.1 \times 4''.2$  ( $1.33 \times 0.78$  kpc<sup>2</sup>) at full width half maximum (FWHM) with P.A.  $\sim -10^\circ$  EofN. This image cube was imported to AIPS for further analysis. In there, Moments 0, 1, and 2 were made using a flux density cutoff of  $2.5\sigma$ , with  $1\sigma \sim 450 \mu\text{Jy beam}^{-1}$  channel<sup>-1</sup>. The H I-line-free 20 cm continuum emission, using the channel ranges 45–75 and 222–240 from all the sessions, was also imaged in CASA using robust=0. The resulting synthesized beam (FWHM) was  $\sim 6''.1 \times 3''.7$  at P.A.  $\sim -8^\circ$  EofN, and the rms noise was  $1\sigma \sim 167.4 \mu\text{Jy beam}^{-1}$ .

To search for extended H I 21 cm cold atomic gas in between NGC 5595 and NGC 5597, we have also made a low resolution image cube using a  $u, v$  range restricted between 0 and 5 k $\lambda$ . This resulted in a synthesized beam (FWHM) of  $\sim 30''.7 \times 28''.8$  at P.A.  $\sim +50^\circ$  EofN, corresponding to a linear resolution of  $\sim 5.4 \times 5.7$  kpc<sup>2</sup>.

### 3. GRAVITATIONALLY BOUND ISOLATED PAIR: NGC 5597 - NGC 5595

The disk galaxies NGC 5595 and NGC 5597 are in the Southern Virgo - Libra Cloud of galaxies, Tully's group 41-14(+14), with a very low galaxy volume density of only 0.16 galaxies Mpc<sup>-3</sup>; see their spatial location at galactic coordinates  $l^{II} \sim 332^\circ.8$ ,  $b^{II} \sim +40.7$  in Plates 1, and 5 (Tully & Fischer 1987), and in  $\alpha$ , and  $\delta$  in Fig. 2 (Tammann 1985).

These two galaxies are separated by  $\Delta\alpha \sim 13^s.54$ ,  $\Delta\delta \sim 138''$  or  $D_{12} \sim 3'.97$  on the plane of the sky. The diameters of NGC 5597 and NGC 5595 are  $d_1 \sim 1'.87$  and  $d_2 \sim 1'.6$ , respectively. Furthermore, these two galaxies have very similar spectroscopic H I 21 cm systemic velocities ( $\Delta V < 5$  km s<sup>-1</sup>). Thus, they indeed satisfy Holmberg's spatial and velocity difference crite-

ria  $\Delta D_{12}/(d_1 + d_2) \ll 2$  (Zwicky 1956; Karachentsev 1972, 1981) indicating that NGC 5597 forms an isolated gravitationally bound pair with the disk galaxy NGC 5595 (Sc).

Figure 1 shows a reproduction of the optical blue continuum 103aO emission from the disk galaxy pair NGC 5597 (SE) and NGC 5595 (NW) in grey scale in relative units taken with the OAN-SPM 2.1m optical telescope in Mexico (Diaz-Hernández et al. 2009). In this blue optical continuum image there are no bridges or structures connecting the two galaxies. In Section 5, it will be shown that there are H I 21 cm extended cold gas structures to the NE and SW of NGC 5595.

### 4. NGC 5597: A LATE TYPE BARRED DISK GALAXY

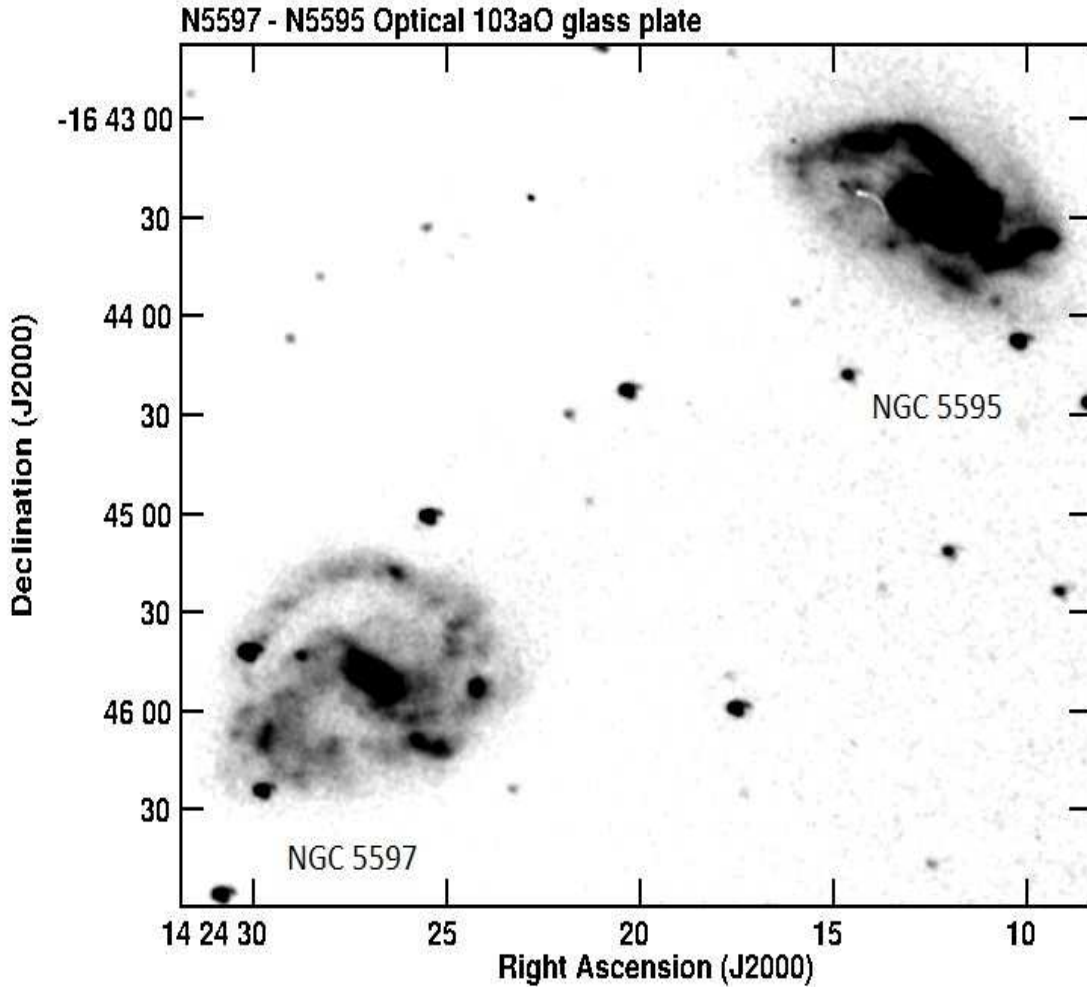
NGC 5597 is a bright ( $m_B \sim 12.57$ ) disk galaxy classified as SBc(s) II (Sandage & Tammann 1981), and as SAB(s)cd, in NED. Table 2 lists the spatial positions of its nucleus estimated from observations at different wavelengths and Table 4 gives its basic properties.

Figure 2 shows a reproduction of the red optical (filter I 8040 Å) of the disk galaxy NGC 5597<sup>4</sup>. Both images of NGC 5597 in Figures 1 and 2 show a central elongated structure about  $2a \sim 28''.3$  by  $2b \sim 14''$  at a P.A.  $\sim 52^\circ$  that we interpret as the boxy stellar bar and have estimated its angular velocity pattern ( $\Omega_{\text{bar}}$ ) (Garcia-Barreto & Momjian 2022).

Additionally, as seen in the SE galaxy in Figure 1, and more specifically in Figure 2, there are at least four narrow and curved structures as spiral arms outside the central region of NGC 5597 (labeled 1 to 4 in Figure 2). The first structure (1) starts from the NE half of the stellar bar and extends to the SE, the second structure (2) starts from the SW of the southern half of the stellar bar and extends further to the SW, the third structure (3) starts from the NW of the southern half of the boxy bar and extends further NW joining the outer fourth structure.

The fourth structure (4) seems to start from the SW of the disk and continues counter clockwise to N, NE, and SE just parallel on the outside of the first structure. A plausible interpretation of the north optical spiral arm in NGC 5597 would be that it is an spiral

<sup>4</sup> The red optical image has not been calibrated in flux density scale, therefore the contours are proportional to the rms noise in relative units.



**Figure 1.** Reproduction of optical blue continuum image (glass plate 103aO) from the close pair of disk galaxies NGC 5597 at the SE and NGC 5595 at the NW, obtained with the OAN-SPM 2.1m optical telescope in Mexico (Díaz-Hernández et al. 2009). The flux density scale has not been calibrated. Grey scale is from  $2 \rightarrow 27.8\sigma$ , where  $\sigma$  is the noise in arbitrary units.

arm near an outer ultraharmonic resonance, UHM<sup>5</sup>  $m=4$  (Contopoulos et al. 1989).

<sup>5</sup> For a star (gas cloud) in a axisymmetric gravitational potential of a disk galaxy,  $\Phi_{\text{disk}}$ , in addition of a weak non-axisymmetric gravitational potential,  $\Phi_{\text{bar}}$ , where  $\Phi_{\text{bar}} \ll \Phi_{\text{disk}}$ , its orbit can be represented as a superposition of the circular motion of a guiding center and small radial oscillations around this guiding center. In cylindrical coordinates with  $z=0$ , the stellar bar gravitational potential may be expressed as  $\Phi_{\text{bar}}(R, \varphi, z=0) = \Phi_b \cos(m\varphi)$ . The equation of motion of a star (gas cloud) is given by the equation of motion of a harmonic oscillator of natural frequency  $\kappa(R)$  that is driven at a frequency  $m(\Omega_{\text{star, gascloud}} - \Omega_{\text{bar}})$ . The solution of the radial motion becomes singular at different values of the guiding center. At corotation radius  $\Omega_{\text{star, gascloud}} = \Omega_{\text{bar}}$ . At other radii  $m(\Omega_{\text{star, gascloud}} - \Omega_{\text{bar}}) = \pm\kappa$ ; for  $m = 2$  the plus and minus signs denote the so called Inner and Outer Lindblad Resonances. When  $m = 4$ , or  $m = 6$  they denote the radii of the so called ultra harmonic resonances (UHM); in particular when  $m = 4$  the minus sign denotes the outer UHM. (Binney & Tremaine 1987; Contopoulos 1988; Contopoulos et al. 1989; Athanassoula 1992)

Figure 3-Left shows our VLA B-configuration HI 21 cm spectrum for NGC 5597. Its overall shape is similar only to the previous Nançay spectrum, because it has the approximate east - west angular resolution to isolate the emission from NGC 5597 (Paturel et al. 2003). The full width of the HI emission line at 20% of the peak, seen in our VLA B-configuration spectrum of NGC 5597, is  $\Delta V_{20\%} \sim 239.25 \text{ km s}^{-1}$  while the full width at 50% of the peak is  $\Delta V_{50\%} \sim 211.40 \text{ km s}^{-1}$  (see Figure 3-left). The Parkes and Green Bank single dish radio telescopes did not have enough angular resolution to separate the two galaxies, resulting in spectra that showed the combined HI 21 cm emission from NGC 5595 and NGC 5597 (Mathewson et al. 1992; Springob et al. 2005). Figure 3-Middle shows the rotation curve of NGC 5597, after several iterations with AIPS task *GAL*, assuming that gas orbits are circular. This rotation curve was ob-

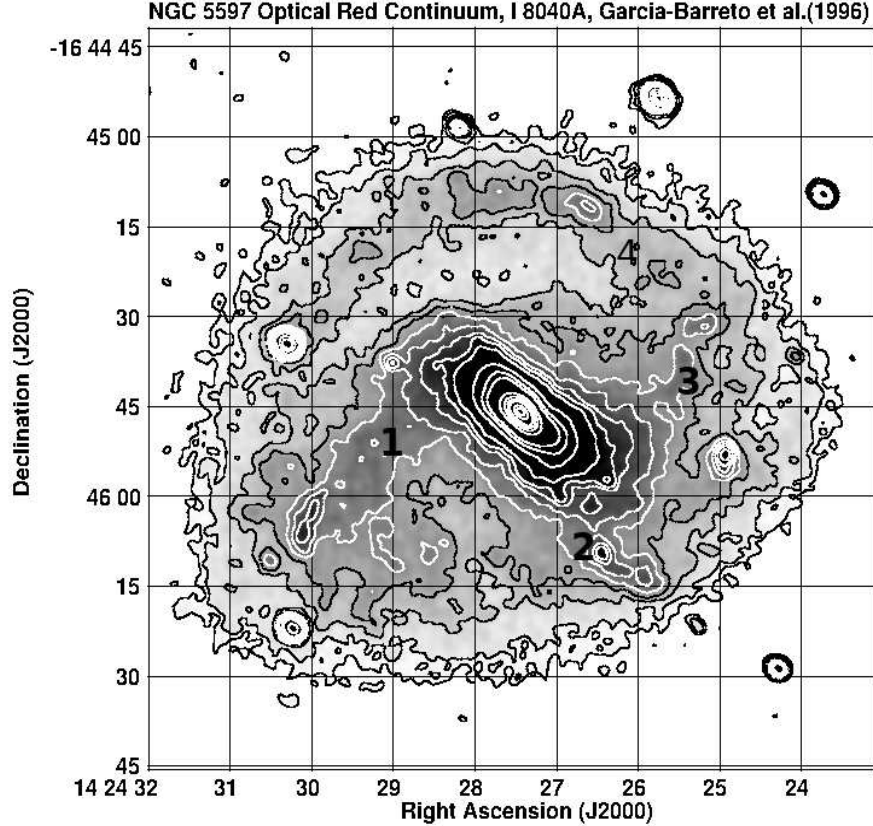


**Figure 2.** Reproduction of optical red continuum image (broadband filter I 8040 Å), in grey scale and contours, of the disk galaxy NGC 5597 obtained with the OAN-SPM 2.1m optical telescope in Mexico (Garcia-Barreto et al. 1996). The image has been convolved with a circular Gaussian beam of  $\sim 1''.5$  at FWHM. The flux density scale has not been calibrated, thus the grey scale stretch is from  $5 \rightarrow 37\sigma$ , where  $1\sigma \sim 45$  is the noise in arbitrary units. Contours are at 5, 7, 11, 15, 20, 25, 30, 34, 40, 60, 80, 100, 200, 300, 400, 500, 750,  $900 \times 1\sigma$ .

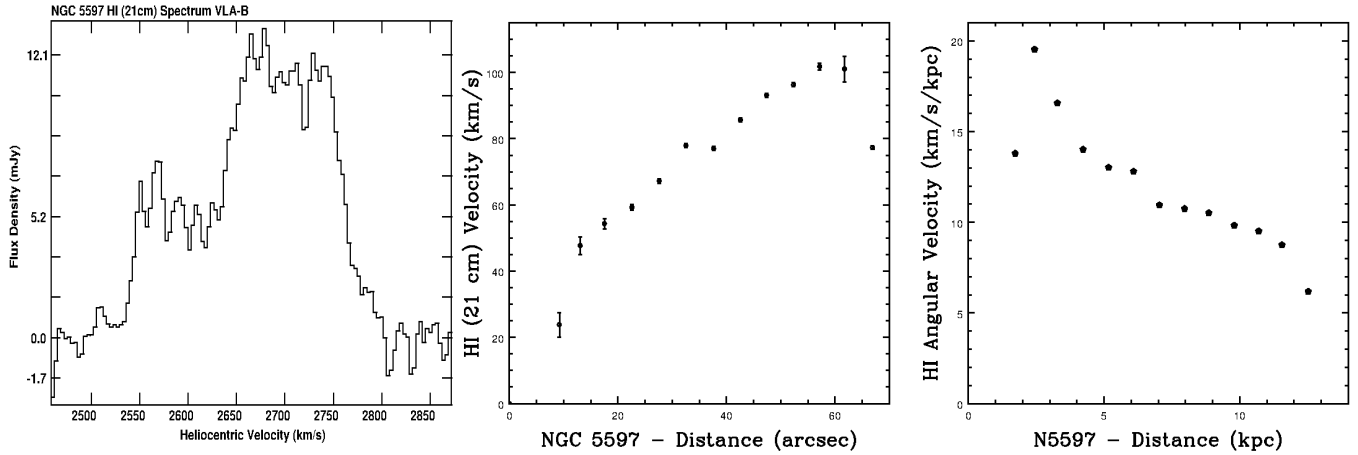
tained in confocal circular anuli each of them  $8''.0$  wide integrated from  $R=0''.0$  up to  $R=70''.0$  with both hemispheres (red and blue shifted velocities compared to the systemic velocity) (Rogstad, Lockhart & Wright 1974). It shows a slowly rising curve with a low velocity value of  $V \sim 24 \text{ km s}^{-1}$  at  $R \sim 9''.23$  ( $\sim 1.73 \text{ kpc}$ ) up to  $V \sim 101 \text{ km s}^{-1}$  at  $R \sim 61''.8$ . The angular velocities curve,  $\Omega_{\text{gas}}$ , shown in Figure 3-Right decreases in such a way that it is less pronounced than a simple  $\Omega_{\text{gas}} \propto 1/(R^{3/2})$ , perhaps suggesting an extended central mass distribution<sup>6</sup>.

#### 4.1. NGC 5597 VLA B-Configuration: Neutral Atomic Gas Spatial Distribution

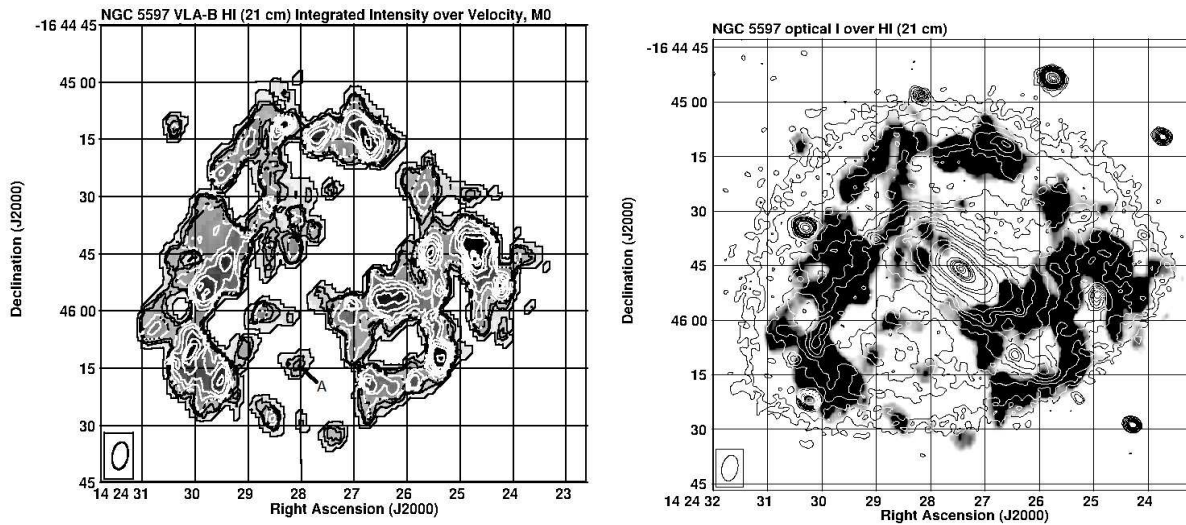
At the angular resolution of our VLA observations (FWHM of  $\sim 7''.1 \times 4''.2$ ), all of the H I 21 cm emission is from within the optical disk of NGC 5597.

Figure 4a shows the H I 21 cm VLA B-configuration integrated intensity over velocity (Moment 0) superposed on itself in grey scale. Figure 4b shows optical I filter image in contours superposed on H I (21 cm) M0 in grey scale. We note that all the H I 21 cm cold gas emission arises from within the optical disk of the galaxy. Notice the narrow, curved and long structures in H I in the NE with an abrupt decrease in emission towards the eastern side. The bright H I cold gas emission from the north lies at a mean distance of  $5.8 \pm 1 \text{ kpc}$  while the optical spiral arm (labeled 4 in Figure 2) lies at a mean distance of  $6.9 \pm 0.94 \text{ kpc}$  on the plane of the sky. Also, there is a weak unresolved peak of H I emission, labeled A in Figure 4a, as if it were the center of a circular area of radius  $\sim 15''$  devoid of H I emission. At that spatial position there is very weak (almost no) optical red emission (see Figure 2). As a comparison, other disk galaxies generally show H I 21 cm gas emission well beyond the optical disk, e.g., M83 (Rogstad, Lockhart & Wright 1974), NGC 1300, SB(rs)bc (England 1989), NGC

<sup>6</sup> Modeling a detailed mass distribution in NGC 5597 is beyond the scope of the present study.



**Figure 3.** Left panel: HI 21 cm spectrum of NGC 5597 obtained from VLA B-configuration observations. The heliocentric systemic velocity, fitted by the task *GAL* in AIPS, is  $V_{\text{helio}}^{\text{(sys)}} = 2698 \text{ km s}^{-1}$ , with  $\Delta V_{50\%} \sim 211.40 \text{ km s}^{-1}$ , and  $\Delta V_{20\%} \sim 239.25 \text{ km s}^{-1}$ . The flux density scale is very difficult to compare to previous Parkes (64 m) and Green Bank (91m) single-dish spectra, because their beam included both disk galaxies NGC 5595 and NGC 5597 (Mathewson et al. 1992; Springob et al. 2005). The shape of the spectrum looks very similar to that obtained with Nançay, however its beam at FWHM was  $\sim 3.6$  east-west  $\times 22'$  north-south (Paturel et al. 2003). Central panel: HI 21 cm rotation curve of NGC 5597. Right panel: HI 21 cm angular velocity curve of NGC 5597.



**Figure 4.** Left: HI 21 cm VLA B-configuration integrated intensity over velocity, Moment 0, image of NGC 5597 in contours superposed on grey scale. The contours are at 3, 35, 50, 70, 100, 125, 150, 175, 200, 250, 270 times  $1\sigma \sim 0.3 \text{ mJy/beam km/s}$ . Greyscale stretch is from  $3\sigma$  to  $200\sigma$ . The synthesised beam at FWHM is shown in lower left corner. Letter *A* indicates an isolated source as if it were in the center of a circular area devoid of HI emission. Right: Optical I filter image in contours (same as Figure 2) over HI (21 cm) M0 in grey scale, with greyscale stretch from 2 to  $17.5 \text{ mJy beam}^{-1} \text{ km s}^{-1}$ .

3783, SBa, (Garcia-Barreto et al. 1999), NGC 3147 S(rs)bc (Haan et al. 2008).

Remarkably in NGC 5597 there is no HI emission from the central region that includes the nucleus and the circumnuclear area. Another area that lacks HI emission is located to the SW of the optical stellar bar and coincides with the odd SW optical spiral arm labeled 2 in Figure 2. It is worth noting that in other disk galaxies (e.g., M31)

HI holes are associated with HII regions (Combes et al. 2002), with hot gas of  $T \sim 10^4 \text{ K}$  (Spitzer 1978), or regions with newly formed stars.

Furthermore, there is no HI cold gas emission from the position of the optical nucleus,  $\alpha(\text{J2000}) = 14^{\text{h}}24^{\text{m}}27^{\text{s}}.49$ ,  $\delta(\text{J2000}) = -16^{\circ}45'45''.9$ , nor from the innermost circumnuclear region where the gas is hot and ionized as indicated by the H $\alpha$  continuum-free

(Garcia-Barreto et al. 1996) and 20 cm radio continuum emission from that region (Condon et al. 1990) and our new VLA B-configuration 20 cm continuum image (see following sections).

#### 4.2. NGC 5597 VLA B-Configuration: Neutral Atomic Gas Velocity Field and Kinematics

Our kinematical analysis of the H I 21 cm emission from NGC 5597 with the task *GAL* in AIPS is presented in Table 5.

Figure 5 shows the velocity field with small redshifted velocities (Left) compared to the systemic velocity of NGC 5597 and with large redshifted velocities (Right). The P.A. of the redshifted semimajor axis is  $\sim 100^\circ$  EofN, with the corresponding P.A. of zero velocities compared to systemic at  $\sim 10^\circ$  EofN.

Figure 6-Left shows the velocity contour lines of the small blueshifted velocities while Figure 6-Right shows the large blue shifted velocity contour lines. To first order, the velocity field indicates a normal disk<sup>7</sup> in differential rotation, with the south-west, SW,  $\rightarrow$  south  $\rightarrow$  south-east, SE,  $\rightarrow$  north-east, NE hemisphere showing redshifted velocities, while the north-east  $\rightarrow$  north  $\rightarrow$  north-west  $\rightarrow$  west hemisphere showing blueshifted velocities.

Taking the P.A.  $\sim 100^\circ$  EofN of the semimajor axis with redshifted velocities in NGC 5597, and assuming the optical spiral arms are trailing, the hemisphere from NW clockwise to SE is closer to the observer with the direction of the axis of rotation projected on the plane of the sky pointing SW at P.A.  $\sim 190^\circ$  EofN. As can be seen in Figure 4-Right, at this angular resolution and sensitivity the H I 21 cm neutral cold gas is confined to the disk.

#### 4.3. NGC 5597 VLA B-Configuration: Neutral Atomic Gas Mass

The total integrated H I flux is,  $\int S_{\text{HI}} dv \sim 2.9$  Jy km s<sup>-1</sup> using the task *IRING* in AIPS with concentric rings, each 8''.0 wide, from  $R = 0''.0 \rightarrow R = 70''.0$  (Rogstad, Lockhart & Wright 1974). The total estimated H I 21 cm atomic hydrogen mass in NGC 5597 is  $M(\text{H I}) \sim 1.02 \times 10^9 M_\odot$ <sup>8</sup>. The dynamical mass in NGC

5597 is  $M_{\text{dyn}} \sim 2.6 \times 10^{10} M_\odot$  as measured from the observed maximum velocity; see Figure 3 Middle panel<sup>9</sup>.

#### 4.4. 20 cm Radio Continuum and H $\alpha$ Emission from NGC 5597

Previous VLA 20 cm radio continuum emission observations of NGC 5597 by Condon et al. (1990) reported an unresolved central structure elongated at P.A.  $\sim 43^\circ$  EofN, see last two values in Table 2.

We have produced a new 20 cm continuum emission image from our VLA B-configuration observing sessions, shown in Figure 7-Right with a restoring beam at FWHM of  $\sim 6''.11 \times 3''.7$  (P.A.  $\sim -8^\circ$  EofN) and contours superimposed on the optical red filter I image of NGC 5597 in grey scale (Garcia-Barreto et al. 1996). Our 20 cm radio continuum image, consistent with previously published images at a similar wavelength (Condon et al. 1990), shows a centrally peaked unresolved structure elongated along P.A.  $\sim 15^\circ$  EofN. The peak flux density of this structure is 9.02 mJy, and the rms noise in the image is  $1\sigma \sim 167.4 \mu\text{Jy beam}^{-1}$ . Additionally, there are at least seven other weaker sources. They are all listed in Table 2 and shown in Figure 7-Right with letters from *a* through *h*.

The total flux density in our 20 cm image is 37 mJy. At the sensitivity of our observations, there is only one 20 cm radio continuum source with a peak flux density of  $3\sigma$  in the optical north-arm labeled *h* but does not coincide with any weak H $\alpha$  source (see Figure 7-Left panel).

Figure 7-Left shows a reproduction of our H $\alpha$ + [N II] continuum-free image of NGC 5597 (Garcia-Barreto et al. 1996) in contours<sup>10</sup> superimposed on the H I 21 cm Moment 0 image in grey scale. The most intense H $\alpha$  emission originates from an unresolved central source with its circumnuclear region and an elongated 13'' structure in P.A.  $\sim 32^\circ \pm 14^\circ$  EofN. Additionally, there are at least seven unresolved H $\alpha$  sources, with low intensity emission in their surrounding associated with the inner optical eastern arm structure (labeled 1 in Figure 2), at least two in the SW optical arm (labeled 2 in Figure 2), extended low intensity emission associated with the optical arm (labeled 3

<sup>7</sup> In a normal disk galaxy in the approximation with only circular orbits ( $v_R = 0$ ,  $v_z = 0$ ) the velocity field will be symmetric about the minor axis and one side will show redshifted velocities compared to the galaxy's systemic velocity, while the other side will show blueshifted velocities; see Fig. 8-17 in (Mihalas & Binney 1981) and Fig. 3.6 in (Combes et al. 2002).

<sup>8</sup> The H I 21 cm total mass in NGC 5597 and later in NGC 5595 was estimated from the known formula  $M(\text{H I}) = 2.356 \times 10^5 D^2 \int S_\nu dV$  where  $D$  is in Mpc,  $S_\nu$  in Jy and  $dV$  is in km s<sup>-1</sup> (Wright 1974)

<sup>9</sup> The dynamical mass is estimated from the known formula resulting from the centrifugal force in circular orbits and the gravitational force from a central massive object, thus one has the expressions for radial forces:  $F_C = mV^2/R$ ,  $F_G = GMm/(R^2)$ . The object (cloud of gas) is in equilibrium of forces, thus when we equal  $F_G$  to  $F_C$  one obtains the expression  $M_{\text{dyn}} = 233.1V^2R$ , where  $V$  is in km s<sup>-1</sup>,  $R$  is in pc, and the mass is in solar masses.

<sup>10</sup> H $\alpha$ + [N II] image was not flux density scale calibrated, thus the contours are proportional to the rms noise in relative units.



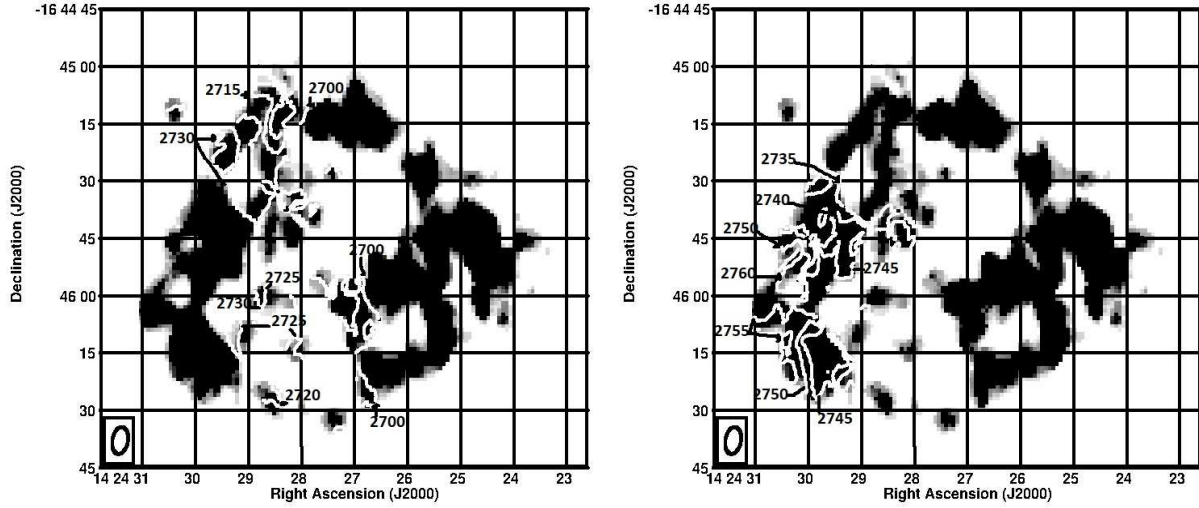


**Figure 5.** Redshifted H I 21 cm velocity field, Moment 1, of NGC 5597 in contours superposed on the Moment 0 grey scale image. The gray scale in both panels ranges from  $1 \text{ mJy beam}^{-1} \text{ km s}^{-1}$  to  $15 \text{ mJy beam}^{-1} \text{ km s}^{-1}$ . Left: The low redshifted velocity contours from center to left are at 2700, 2705, 2710, 2715, 2720, 2725 and 2730  $\text{km s}^{-1}$ . Right: The high redshifted velocity contours from center to left are at 2735, 2740, 2745, 2750, 2755, and 2760  $\text{km s}^{-1}$ .

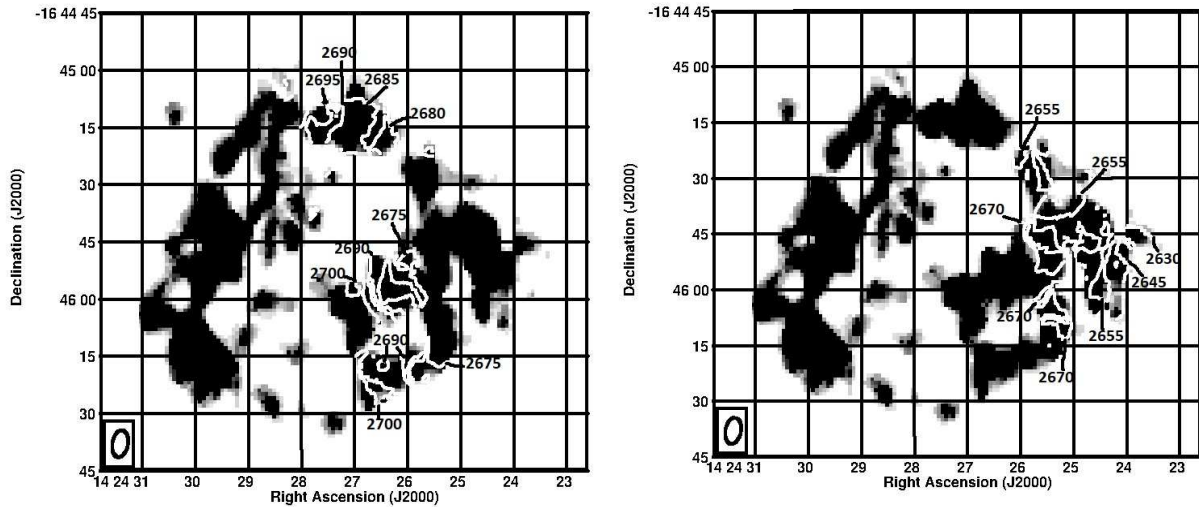


**Figure 6.** Blueshifted H I 21 cm velocity field, Moment 1, of NGC 5597 in contours superposed on the Moment 0 grey scale image. The gray scale ranges from  $1 \text{ mJy beam}^{-1} \text{ km s}^{-1}$  to  $15 \text{ mJy beam}^{-1} \text{ km s}^{-1}$ . Left: the low blueshifted velocity contours from center to right are at 2700, 2695, 2690, 2685, 2680, and 2675  $\text{km s}^{-1}$ . Right: The high blueshifted velocity contours from center to right are at 2670, 2665, 2660, 2655, 2650, 2645, 2640, 2635, 2630, 2625 and 2620  $\text{km s}^{-1}$ .

in Figure 2) and at least 9 unresolved sources associated with the north arm (labeled 4 in Figure 2). The peak

of the bright H $\alpha$  emission from the north optical arm (labeled 4) is at slightly larger distance than the peak of the H I 21 cm emission in that arm.

**Table 2.** Spatial Positions of the Nucleus in NGC 5597 measured in various Bands/Images, and the positions of other 20 cm continuum sources in NGC 5597

Image	$\alpha$ (J2000)	$\delta$ (J2000)	Source	Reference
name	<i>hh mm ss.ss</i>	<i>° ' "</i>		
(1)	(2)	(3)	(4)	(5)
103aO	14 24 27.49	-16 45 45.9	nucleus	1
I	14 24 27.44	-16 45 45.9	nucleus	2
H I 21cm	14 24 27.16	-16 45 46.64	nucleus	3
H $\alpha$	14 24 27.34	-16 45 47.39	peak of emission	2
20 cm cont.	14 24 27.40	-16 45 46.00	nucleus <sup>a</sup>	3
20 cm cont	14 24 28.03	-16 45 48.00	E on disk <sup>b</sup>	3
20 cm cont	14 24 29.07	-16 45 40.00	NE on disk <sup>c</sup>	3
20 cm cont	14 24 29.91	-16 46 04.00	SE on disk <sup>d</sup>	3
20 cm cont	14 24 27.47	-16 46 06.00	S on disk <sup>e</sup>	3
20 cm cont	14 24 26.36	-16 45 49.00	W on disk <sup>f</sup>	3
20 cm cont	14 24 24.97	-16 45 49.00	W on disk <sup>g</sup>	3
20 cm cont	14 24 28.40	-16 45 07.00	N on disk <sup>h</sup>	3
old 20 cm	14 24 27.45	-16 45 45.27	nucleus	4
old 20 cm	14 24 27.35	-16 45 45.27	nucleus	4

<sup>a</sup> 53.9 $\sigma$ , <sup>b</sup> 6.7 $\sigma$ , <sup>c</sup> 4.2 $\sigma$ , <sup>d</sup> 3.8 $\sigma$ , <sup>e</sup> 4.2 $\sigma$ , <sup>f</sup> 4.3 $\sigma$ , <sup>g</sup> 4.1 $\sigma$ , <sup>h</sup> 3 $\sigma$  where  $1\sigma \sim 167\mu\text{Jy}/\text{beam}$ . These peaks of the 20 cm continuum sources are labeled *a* through *h* in Figure 7-Right.

NOTE—1) (Diaz-Hernández et al. 2009), 2) (Garcia-Barreto et al. 1996), 3) This work, 4) (Condon et al. 1990)

NOTE—The first old 20 cm radio continuum position by Condon et al. (1990) was with a circular beam FWHM $\sim 21''$ . The second old position was with a circular beam FWHM $\sim 7''$ .

The lack of cold atomic H I 21 cm emission in the inner 20'' together with the presence of extended hot gas<sup>11</sup> in a P.A. similar to the P.A. of the rotation axis of the galaxy may indicate the presence of a low velocity bipolar outflow. While this extended hot gas might also be the result of central star formation, explaining its P.A. as seen in both H $\alpha$  and 20 cm radio continuum would be a challenge.

All of H $\alpha$  sources throughout the disk indicate regions of massive O and B star formation with ionization and recombination processes of atomic hydrogen (Spitzer 1978) with hot gas,  $T \sim 10^4$  K, extending out of the plane of the galaxy. The temperature of the H I 21 cm gas presented in this paper, however, corresponds to an H I spin temperature of  $T_s \leq 100$  K (Purcell & Field 1956; Field 1958a,b; Wright 1974; Spitzer 1978; Combes et al. 2002). Assuming the neu-

tral gas distribution in NGC 5597 is similar to that in our galaxy, the H I 21 cm cold gas and sodium, Na I, are constituents of diffuse neutral clouds in a thin layer on the plane of the galaxy's disk (Spitzer 1978) with thickness probably less than 200 pc (Burton 1974).

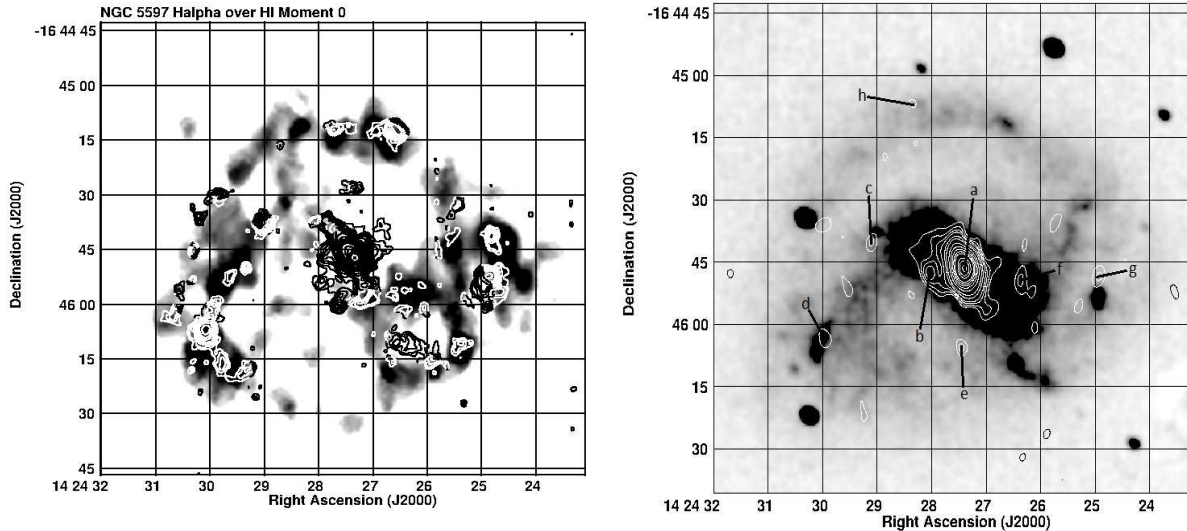
#### 4.5. Central 20'' Gas Emission from NGC 5597

Figure 8-Right shows the central innermost  $\sim 20''$  image of our new 20 cm continuum emission in contours obtained with the VLA in B-configuration. The image is superposed on the grey scale image of the H I 21 cm Moment 0 of NGC 5597. The peak of the 20 cm continuum emission at this angular resolution (FWHM of  $\sim 6''.11 \times 3''.7$ , P.A.  $\sim -8^\circ$ ) coincides fairly well with the position of the nucleus seen in the blue optical 103aO and the red optical (I filter) images. Table 2 list the positions of the center or nucleus<sup>12</sup> in NGC 5597 and they are also shown with different symbols in Figure 8.

The new 20 cm radio continuum map shows that the emission arises from an unresolved source with an elongated structure in the NE-SW direction at P.A.  $\sim 17 \pm 7^\circ$

<sup>11</sup> By hot gas we mean gas from synchrotron plus thermal processes from observed H $\alpha$  and 20 cm radio continuum optically thin emissions that indicate  $T_e \sim 10^4$  K.

<sup>12</sup> H I 21 cm kinematic, photometric 103aO and I optical filters.



**Figure 7.** Left: reproduction of the  $H\alpha$  line emission image of NGC 5597 (Garcia-Barreto et al. 1996) in contours superimposed on the H I 21 cm Moment 0 in grey scale. The  $H\alpha$  image is not calibrated in flux density scale, therefore the contours are proportional to noise in arbitrary units from  $3.5\sigma$  to  $17\sigma$ . The most intense central emission of the hot gas, seen in  $H\alpha$ , is devoid of cold gas H I 21 cm emission. At least two  $H\alpha$  sources are offset by a few arcsec to the north of the H I 21 cm sources. Right: Our new 20 cm radio continuum emission image in contours superimposed on the optical red (I filter 8040 Å) image (Garcia-Barreto et al. 1996). The restoring beam size of the 20 cm continuum image at FWHM is  $\sim 6''.11 \times 3''.7$  (P.A.  $\sim -8^\circ$ ). The contours are from 3, 4, 5, 6, 8, 10, 14, 18, 22, 26, 30, 40, 45 and  $53\sigma$  where  $1\sigma \sim 167.4 \mu\text{Jy beam}^{-1}$ . The strongest 20 cm radio continuum emission arises from an unresolved source coincident with the position of the optical nucleus with an inner elongated structure at a P.A.  $\sim 25^\circ$  EofN. The peaks of 20 cm continuum sources are labeled *a* through *h* as listed in Table 2.

EofN, This elongation is very comparable to the galaxy’s rotation axis projected on the plane of the sky (direction P.A.  $\sim 190^\circ$  EofN or orientation P.A.  $\sim 10^\circ$  EofN). This NE-SW 20 cm radio continuum elongation is a true physical orientation and not due to a beam elongation artifact (since the beam P.A.  $\sim -8^\circ$  EofN). Also, it is in a similar orientation as the elongated structure seen in  $H\alpha$ , which we discuss further below.

The observed 20 cm continuum emission is a mixture of synchrotron process with high velocity electrons interacting with an external magnetic field,  $\vec{B}^{13}$ , and thermal process (free free optically thin) with a typical electron temperature of  $T_e \sim 10^4$  K from H II regions and/or supernova processes<sup>14</sup>.

Figure 8-Left shows in contours the  $H\alpha + [\text{N II}]$  continuum-free line emission, superposed on the grey scale VLA B-configuration H I 21 cm Moment 0 map.

Similar to the 20 cm radio continuum emission, the  $H\alpha$  emission in the center of the galaxy originates from an unresolved source with an elongated structure in the NE-SW direction at P.A.  $\sim 32 \pm 14^\circ$  or P.A.  $\sim 212 \pm 14^\circ$ . This  $H\alpha$  emission comes from a recombination line process in the innermost H II circumnuclear region.

Both the central  $H\alpha$  and 20 cm radio continuum emissions are elongated in the NE - SW direction and qualitatively their spatial extension is similar. The stellar bar (in the optical red, I, filter) lies at P.A.  $\sim 52^\circ$  and rotates at  $\Omega_{\text{bar}} \sim 15.3 \text{ km s}^{-1} \text{ kpc}^{-1}$  (Garcia-Barreto et al. 1996; Garcia-Barreto & Momjian 2022). In that central region there is no H I 21 cm emission. Furthermore, the spatial distribution of both the hot gas, seen in  $H\alpha$ , and the thermal/synchrotron 20 cm radio continuum suggests a bipolar geyser<sup>15</sup> into the innermost NE - SW direction with additional emission from an innermost circumnuclear region.

<sup>13</sup> For optically thin synchrotron emission,  $S_\nu \propto B_\perp^{1.75} \nu^{-0.75} \theta^3$ , while the free-free emission for an optically thin case,  $S_\nu \propto T_e^{-0.35} \nu^{-0.1} EM$ .

<sup>14</sup> Future VLA radio continuum observations of NGC 5597 at a higher angular resolution and polarization analysis would be critical to better understand the physical mechanisms and the  $\vec{E}$  (and  $\vec{B}$ ) orientation.

<sup>15</sup> The term ‘geyser’ is utilized as a synonym to low velocity (hundreds of  $\text{km s}^{-1}$ ) extragalactic nuclear outflow (Moody et al. 1995). In contrast, extragalactic plasma outflows, like in M87, have much higher velocities (many thousands of  $\text{km s}^{-1}$ ) (Reid et al. 1989).

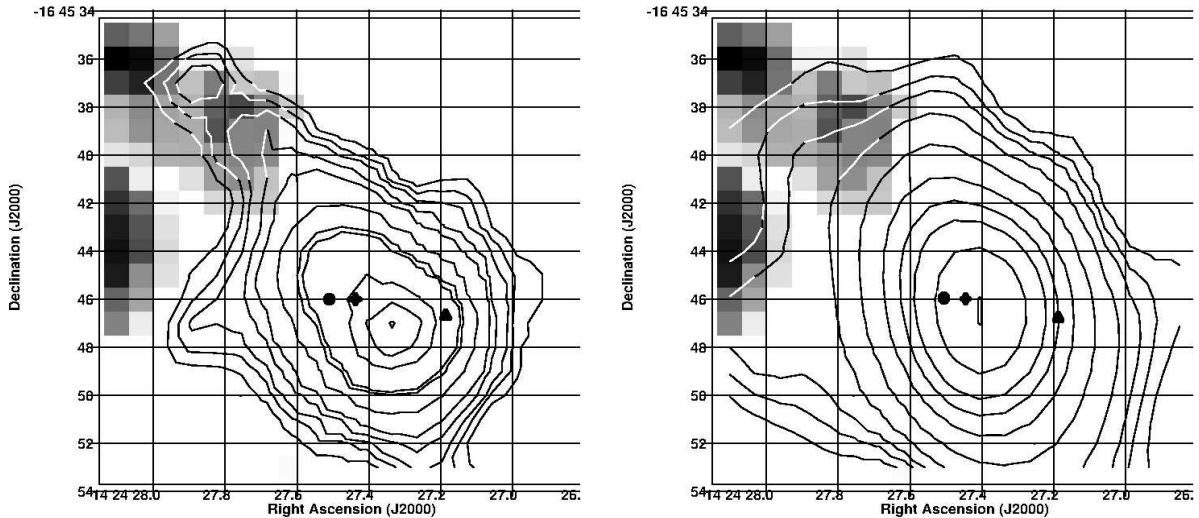


**Figure 8.** Innermost  $20''$  of NGC 5597, the filled triangle shows the kinematical center of H I 21 cm emission, the four point star shows the position of the photometric optical red I filter image, and the filled circle shows the position of the photometric blue 103aO image. Spatial coordinates are listed in Table 2. Left: H $\alpha$  continuum-free emission in contours superposed on VLA B-configuration H I 21 cm Moment 0 image in grey scale. The optical image is not calibrated in flux density scale, and the contour levels are at 7, 9, 11, 15, 20, 40, 80, 100, 300, 500, and 720 times  $1\sigma$  where  $1\sigma = 10$  in relative units. Grey scale ranges from 5.76 to 30 mJy beam $^{-1}$  km s $^{-1}$ . The extended emission lies at P.A.  $\sim 32^\circ \pm 14^\circ$ . Right: our new VLA B-configuration 20 cm continuum emission in contours superposed on the H I 21 cm MOM 0 image in grey scale. The contour levels are the same as in Figure 8b. The NE extended 20 cm radio continuum is in P.A.  $\sim 17^\circ \pm 7^\circ$ . Grey scale ranges from 5 to 25 mJy beam $^{-1}$  km s $^{-1}$ . Notice that the peak of the H $\alpha$  emission (left panel) is slightly south-west from the peak of the 20 cm radio continuum (right panel) that is associated with the optical nucleus. Qualitatively both the 20 cm continuum and the H $\alpha$  spatial emissions are similar. There is no cold gas atomic H I 21 cm emission (in grey scale) from the nucleus and the innermost circumnuclear region.

In both images in Figure 8 the H I 21 cm emission, shown in grey scale, is only seen from the extreme NE of the central  $20''$  region of NGC 5597. The peak of the H $\alpha$  emission lies slightly south-west of the optical photometric position of the nucleus (see Table 2). Although the small difference in these two positions might be due to astrometry, it might well be the correct spatial position of the SW H $\alpha$  emission (brightest) from a bipolar nuclear geyser as observed clearly in the barred disk galaxy NGC 1415 where there is weak or no H $\alpha$  emission from the optical nucleus but two bright unresolved H $\alpha$  sources from the lobes of a geyser (Garcia-Barreto et al. 1996; Garcia-Barreto & Moreno 2000; Garcia-Barreto et al. 2019). In this scenario, the NE lobe of such an H $\alpha$  bipolar geyser or outflow in NGC 5597 might also exist, however, our image does not have the proper angular resolution to reveal it, especially that the emission is mixed with the elongated structure in the NE-SW direction (see Figure 7-left).

If the H $\alpha$  and the 20 cm radio continuum emission from NGC 5597 do indeed indicate a bipolar geyser or nuclear outflow, the hot ionized gas and the relativistic electrons would be out of the plane of rota-

tion of this galaxy, similar to e.g., the large lobes seen in radio continuum in the barred galaxy NGC 3367 (Garcia-Barreto et al. 1998, 2002).

Although we are not yet aware of any published work on molecular gas emission in NGC 5597, one may expect a total  $M(H_2) \sim 6.4 \times 10^9 M_\odot$  from the CO - FIR correlation (Scoville 1988). For example, molecular gas emission has been observed from the innermost central regions of two nearby bright barred galaxies like NGC 1068 (Planesas et al. 1991) where there is a nuclear bipolar radio continuum emission (van der Hulst et al. 1982; Wilson & Ulvestad 1987) and NGC 3367 (Garcia-Barreto et al. 1998, 2002, 2005).

From the literature, there are many normal disk or barred galaxies with weak active galactic nuclei, such as the following four examples: a) M51, SA(s)bc pec, is a normal disk galaxy with a central mild activity that indicates the presence of a bidirectional jet, shown by H $\alpha$  + N[II] monochromatic image, optical red spectra, and radio continuum emission associated with the central region emanating from the nucleus as seen in high angular resolution VLA observations

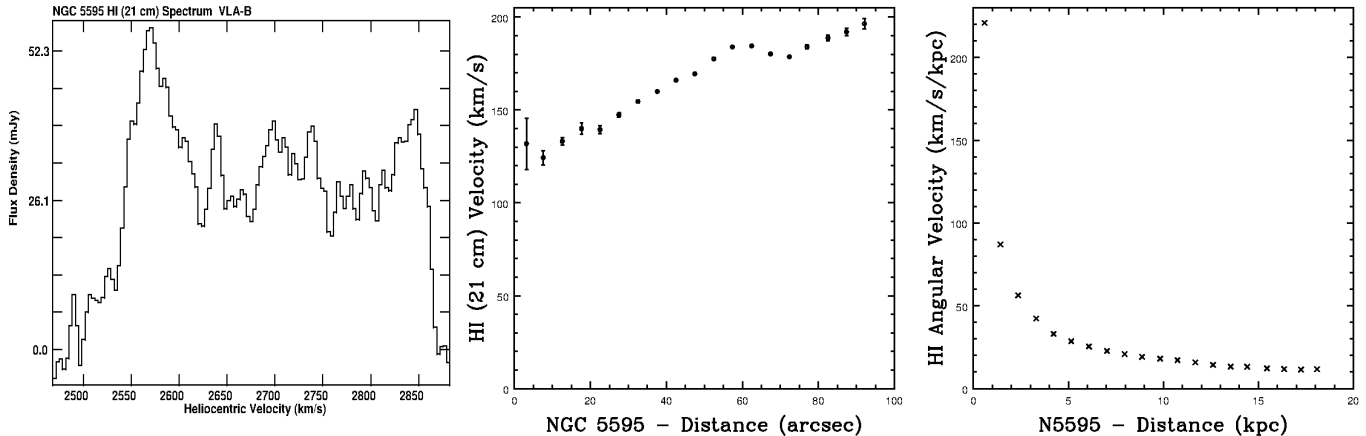


**Figure 9.** Left: H I 21 cm spectrum obtained from our VLA B-configuration observations of the disk galaxy NGC 5595. The heliocentric systemic velocity, fitted by the task *GAL* in AIPS, is  $V(\text{sys})_{\text{helio}} = 2702 \text{ km s}^{-1}$ , with  $\Delta V_{50\%} \sim 317.5 \text{ km s}^{-1}$ , and  $\Delta V_{20\%} \sim 345 \text{ km s}^{-1}$ . The flux density scale of the spectrum is very difficult to compare to previous ones obtained with Parkes (64 m) and Green Bank (91m) radio telescopes because their beam included both disk galaxies NGC 5595 and NGC 5597 (Mathewson et al. 1992; Springob et al. 2005). The shape of the spectrum looks very similar to that obtained with Nançay, however its beam at FWHM was  $\sim 3'6$  east-west  $\times 22'$  north-south (Paturel et al. 2003). Middle: NGC 5595 H I 21 cm rotation curve. Right: NGC 5595 H I 21 cm angular velocity  $\Omega_{\text{gas}}$ .

(Ford et al. 1985; Cecil 1988; Crane & van der Hulst 1992). Furthermore, there is dense molecular gas in the inner  $\leq 50 \text{ pc}$  of M51 located in two blobs at a P.A.  $\sim 75^\circ$ , perpendicular to the elongation of the optical  $\text{H}\alpha$ , and radio continuum images (Scoville et al. 1998); b) NGC 1068, Sb(rs) II (Sandage & Tammann 1981), with a stellar bar (Scoville 1988), central molecular gas (Planesas et al. 1991), and a bipolar radio continuum nuclear source (Wilson & Ulvestad 1987); NGC 1415, SBa (Sandage & Tammann 1981) with two bright  $\text{H}\alpha$  unresolved sources straddling the nucleus labeled A to the south-east and B to the north-west (Garcia-Barreto et al. 2019) which may be the result of a bipolar geyser with  $v_{\text{rm,geyser}} \sim 140 \text{ km s}^{-1}$  and d) NGC 3367, SBc(s) II (Sandage & Tammann 1981), with central molecular gas (Garcia-Barreto et al. 2005), central  $\text{H}\alpha$  emission (Garcia-Barreto et al. 1996), and a bipolar radio continuum source (Garcia-Barreto et al. 1998, 2002).

If one takes the velocity dispersion of stars in the innermost central region of each galaxy from the published literature (Ho et al. 2009), and use the  $M_{\text{BH}} - \sigma_*$  correlation relation (Gebhardt et al. 2000; Merritt & Ferrarese 2001a,b), then the mass of the super massive black hole (SMBH) in each of these three barred galaxies are:  $M_{\text{NGC1068-BH}} \sim 9.7 \times 10^7 M_\odot$ ,  $M_{\text{M51-BH}} \sim 7.6 \times 10^6 M_\odot$ , and  $M_{\text{NGC3367-BH}} \sim 1.4 \times 10^6 M_\odot$ . Thus, the observed central  $\text{H}\alpha$  emission, the 20 cm radio continuum emission, and the central H I 21 cm hole, in all of these barred galaxies may indeed be the result of a central SMBH.

As a comparison, the masses of the SMBH in two normal disk galaxies observed with nuclear geysers or bipolar outflows, namely M81 (NGC 3031; Sb(r)I-II) and M101 (NGC 5457, Sc(s) I), using the same  $M_{\text{BH}} - \sigma_*$  correlation, are:  $M_{\text{M81-BH}} \sim 5.4 \times 10^7 M_\odot$  and  $M_{\text{M101-BH}} \sim 3.97 \times 10^4 M_\odot$ , respectively (Garcia-Barreto et al. 2019).

In the case of the barred galaxy NGC 5597, one of the two galaxies in this study, the central observed distribution of the  $\text{H}\alpha$  emission, the 20 cm radio continuum emission, and the H I 21 cm hole, all seem to suggest the existence of a SMBH with  $M_{\text{NGC5597-BH}} \sim 10^6 M_\odot$ .

## 5. NGC 5595: A LATE TYPE DISK GALAXY

### 5.1. General Characteristics

NGC 5595 is classified as Sc(s)II (Sandage & Tammann 1981), SAB(rs)c (de Vaucouleurs et al., RC3, 1993). It is a member of a close pair with NGC 5597 to the SE at a projected angular distance on the plane of the sky of  $\sim 3'97$  (Garcia-Barreto, Carrillo, & Villamizar 2003). As mentioned earlier in the case of NGC 5597, they both have very similar systemic velocities and are close on the plane of the sky, therefore we also adopt its distance as  $D_{\text{pair}} = 38.6 \text{ Mpc}$  (Tully 1988) ( $1'' \sim 187.14 \text{ pc}$ ). Figure 1 shows its blue continuum optical emission from our 103aO observation (Diaz-Hernández et al. 2009). As in the case of NGC 5597, astrometry was done to independently estimate its photometric position (Diaz-Hernández et al. 2009). See Table 4 for its basic properties.

### 5.2. VLA B-Configuration H I 21 cm Observations

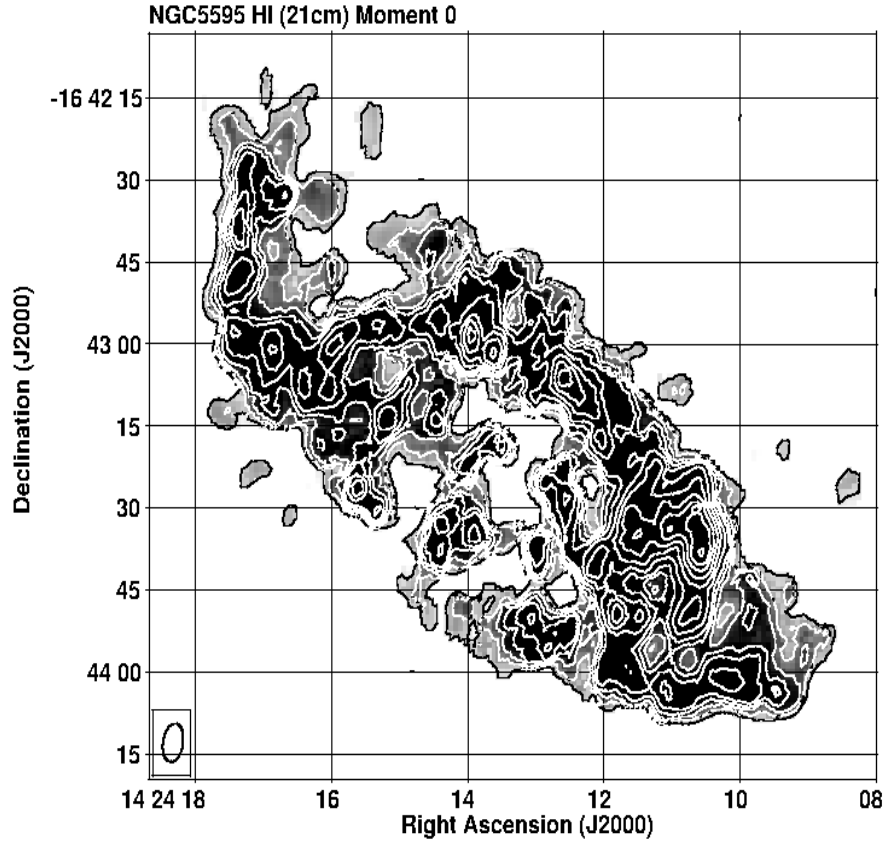


**Figure 10.** NGC 5595 VLA B-configuration HI 21 cm integrated intensity over velocity, Moment 0, image in grey scale and contours. The contour levels are at  $3, 6, 9, 12, 15, 20, 25, 30, 35, 40$  and  $47 \times 1\sigma = 3.3 \text{ Jy beam}^{-1} \text{ km s}^{-1}$ . Notice that there is no atomic hydrogen gas emission from the position of the kinematical center  $\alpha(\text{J2000.0}) = 14^{\text{h}}24^{\text{m}}13^{\text{s}}.3$ ,  $\delta(\text{J2000.0}) = -16^{\circ}43'21''.6$ . This position coincides with the optical continuum photometric center. The VLA B-configuration beam size, which is  $\sim 7''.14 \times 4''.21$  at FWHM, is shown in the lower left corner.

As previously discussed in the section on NGC 5597, the Parkes and Green Bank single dish radio telescopes did not have enough angular resolution to separate the two galaxies, resulting in spectra that showed the combined HI 21 cm emission from both NGC 5595 and NGC 5597 (Mathewson et al. 1992; Springob et al. 2005). Only the Nançay radio telescope, with a FWHM beam size of  $\sim 3''.6$  east-west  $\times 22''$  north-south, was able to isolate the HI 21 cm emission spectrum of NGC 5595 with a peak flux density of  $\sim 100 \text{ mJy}$  and a velocity range  $\sim 2525 \rightarrow 2875 \text{ km s}^{-1}$  (Paturel et al. 2003).

Figure 9-Left panel shows our VLA B-configuration HI 21 cm spectrum from NGC 5595 using task *ISPEC* in AIPS. The shape is very similar to the Nançay spectrum (Paturel et al. 2003). Using the AIPS task *GAL*, the fitted kinematic HI 21 cm systemic velocity is  $V_{\text{sys}} \sim 2702 \text{ km s}^{-1}$  using both redshifted and blueshifted velocities. The measured velocity widths in the spectrum obtained from our VLA B-configuration observations are

$\Delta V_{50\%} \sim 317.5 \text{ km s}^{-1}$  and  $\Delta V_{20\%} \sim 345 \text{ km s}^{-1}$  at 50% and 20%, respectively. Figure 9-Middle panel shows the rotation curve from NGC 5595 from our fit assuming circular orbits (Rogstad, Lockhart & Wright 1974). It has a high value from a small radius then decreases a little bit then continues slowly rising all the way until  $90''$ . Finally, Figure 9-Right panel shows the NGC 5595 angular velocity ( $\Omega_{\text{gas}} \equiv V(R)/R$ ); notice its very smooth decreasing values.

### 5.3. HI 21 cm Spatial Distribution and Kinematics

Figure 10 shows the VLA B-configuration HI 21 cm velocity integrated Moment 0 map from NGC 5595 in contours superimposed on itself on grey scale. Most of the emission originates from giant HI 21 cm clouds in normal differential rotation around the nucleus of the disk galaxy. The spatial extent of the HI 21 cm emission spans  $\Delta \text{R.A.} \sim 18^{\text{s}} \rightarrow 09^{\text{s}}$  and  $\Delta \text{Dec} \sim -16^{\circ}42'15'' \rightarrow -16^{\circ}44'10''$ . Notice that the optical north spiral arm

in NGC 5595 is assumed to be trailing (e.g., Figure 1). However, the NE HI 21 cm extended morphology, on the plane of the sky, appears as if it were a leading structure<sup>16</sup>.

We also note the lack of HI 21 cm emission from the central region, where there seems to be a circumnuclear radio continuum structure (see subsection 5.5).

Figure 11 shows our VLA B-configuration HI 21 cm velocity field. The kinematical parameters are listed in Table 3. The Left panel shows the contours of the blueshifted velocities (compared to systemic velocity), while the Right panel shows the contours of the redshifted velocities from center to SW. The NE  $\rightarrow$  N  $\rightarrow$  SW hemisphere is closer to the observer, and the projection on the plane of the sky for the orientation of the rotation axis of the disk galaxy is at P.A.  $\sim$  327 EofN, with a direction pointing to the NW.

Figure 10 reveals (as well as Figures 11 and 12) for the first time the existence of extended HI 21 cm cold gas structures to the NE and SW of the disk galaxy NGC 5595 with no blue optical continuum nor 20 cm radio continuum counterparts. The approximate length of the HI 21 cm tails at the NE and the SW of NGC 5595 on the plane of the sky are  $\sim$  7 kpc and  $\sim$  4.2 kpc respectively. The NE contours show blueshifted velocities as if they were a smooth continuation of the blueshifted velocities from the inner disk. Similarly, the lower-most SW contours show redshifted velocities as if they were a smooth continuation of the redshifted velocities from the inner disk. Both (NE & SW) extended structures seem to be warps of the NGC 5595 disk<sup>17</sup>.

Figure 12 shows the reproduction of the blue optical continuum 103aO emission from NGC 5595 in contours (Diaz-Hernández et al. 2009) superposed on the HI 21 cm Moment 0 map in grey scale (see Figure 10). The blue optical image is not flux calibrated, so the contours are proportional to  $1\sigma$  noise level in arbitrary units.

As mentioned earlier, the NE HI 21 cm extension morphology is peculiar since it shows blueshifted velocities and it appears, on the plane of the sky, as if it were a leading structure; the north optical (blue) spiral arm is assumed to be trailing and shows also blueshifted velocities. The NE and SW HI 21 cm elongated emissions may be filamentary gas structures that are most likely a result of a recent gravitational tidal interaction with its neighbor NGC 5597. Similar extended structures have

been observed in the M82 galaxy (Yun, Ho & Lo 1993), and have been shown to exist from computer simulations (Toomre & Toomre 1972; Mihos & Hernquist 1996).

#### 5.4. NGC 5595: Cold Hydrogen Atomic Gas Mass

The total HI 21 cm gas mass in NGC 5595 is  $M(\text{HI}) \sim 2.9 \times 10^9 M_\odot$ . The dynamical mass in NGC 5595 is  $M_{\text{dyn}} \sim 1.3 \times 10^{11} M_\odot$  as measured from the observed maximum velocity; see Figure 9-Middle panel.

#### 5.5. NGC 5595: Our VLA B-configuration 20 cm Radio Continuum Emission Map

Previously published 20 cm VLA radio continuum observations with an angular resolution of  $\sim 21''$  at FWHM showed an unresolved central source in NGC 5595 elongated into the NE - SW orientation (Condon et al. 1990), while at an angular resolution of  $\sim 7''$  at FWHM the VLA image showed also an unresolved central source with at least three other weaker peaks of emission and weak extended emission surrounding them. All the 20 cm radio continuum emission reported arise from the disk of NGC 5595 (Condon et al. 1990).

We have produced a new 20 cm radio continuum emission image from our VLA B-configuration observations with an angular resolution of  $\sim 6''.11 \times 3''.7$  at FWHM (P.A.  $\sim -8^\circ$  EofN). This continuum image is shown in Figure 13 in contours superimposed on the reproduction of the blue optical continuum 103aO image in grey scale. The 20 cm continuum image shows an unresolved dominant central source with a peak flux density of 2.59 mJy at  $\alpha \sim 14^h 24^m 13^s 203$ ,  $\delta \sim -16^\circ 43' 21''.99$ . This position coincides with the photometric blue optical continuum 103aO nucleus and the kinematic HI 21 cm center (see Tables 1 and 4). Additionally, there are other 20 cm continuum sources in what seems a circumnuclear region within an angular distance from the nucleus  $R_{\text{N-CNR}} \sim 9''.5$  or within a linear distance  $R_{\text{N-CNR}} \sim 1.77$  kpc. There are also 20 cm continuum sources associated with the north and SW spiral arms within the disk. The total 20 cm radio continuum flux density in our new image obtained with the VLA in B-configuration is  $\sim 81.83$  mJy.

Our new VLA B-configuration 20 cm radio continuum image shows that, at the sensitivity of the observations, all the 20 cm radio continuum emission originates from the optical disk of NGC 5595 (see Figure 13). At the position of the unresolved dominant central 20 cm radio continuum emission there is no HI 21 cm neutral cold gas emission (see Figures 10). The origin of the 20 cm radio continuum emission is most likely a mixture of thermal ( $T_e \sim 10^4$  K) and optically thin synchrotron

<sup>16</sup> This could be a plausible result of a flat retrograde parabolic passage of a companion of equal mass, see Fig. 1 t = 4 in Toomre & Toomre (1972).

<sup>17</sup> The large scale warps of disk galaxies remain a challenge for theorists (Toomre 1983).

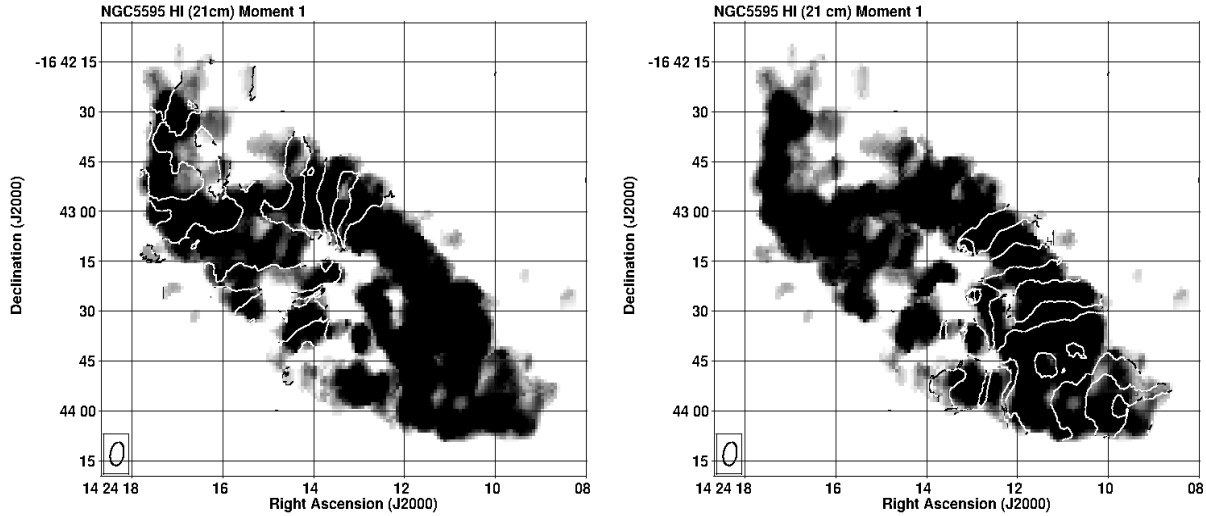


**Figure 11.** Left panel shows the H I 21 cm velocity field of NGC 5595, MOM 1, with blueshifted velocities in contours superposed on Moment 0 image in grey scale (scale stretch is from  $7.7 \text{ mJy beam}^{-1} \text{ km s}^{-1}$  to  $37 \text{ mJy beam}^{-1} \text{ km s}^{-1}$ ). Velocity contours from center to NE are at 2690, 2670, 2650, 2630, 2610, 2590, 2570, 2560 and  $2550 \text{ km s}^{-1}$ . Right panel shows the redshifted velocity contours from center to SW are at 2700, 2720, 2740, 2760, 2780, 2800, 2820, 2840, 2850 and  $2855 \text{ km s}^{-1}$ . The velocity field indicates differential rotation as expected from a disk galaxy. Notice that the upper-most NE contours show blueshifted velocities as if they were a smooth continuation from the blueshifted velocities from the inner disk, although the cold atomic H I 21 cm gas there has no optical counterpart. Similarly the SW contours show redshifted velocities as if they were a smooth continuation from the redshifted velocities from the inner disk, although the cold atomic H I 21 cm gas there has no optical counterpart.

processes related to star formation (H II regions) and their evolution (supernovas). There are no 20 cm radio continuum emission from the upper-most NE and the lower-most SW structures that exhibit H I 21 cm emission as seen in the Moment 0 image (see Figures 10, 11 and 12).

#### 6. NO TIDAL FILAMENTARY STRUCTURES IN BETWEEN THE FIELD OF THE PAIR DISK SYSTEM NGC 5595 AND NGC 5597

The isolated galaxy pair NGC 5597 - NGC 5595 is in an area of the universe with very low galaxy volume density (Tammann 1985; Tully & Fischer 1987), therefore, there is no hot intergalactic gas which could have stripped the atomic gas from outer disk radii. Thus, it seems that both NGC 5595 and NGC 5597 originated with just enough H I atomic neutral gas to form their disks and stars.

**Table 3.** Kinematical H I 21 cm VLA B-configuration Analysis of the Disk Galaxy Pair NGC 5595 and NGC 5597

Galaxy name	$\alpha(\text{J2000})$ <i>hh mm ss.ss</i>	$\delta(\text{J2000})$ $^{\circ} \ ' \ ''$	Position Angle <sup>a</sup> $^{\circ}$ EofN	Inclination $^{\circ}$	$V(\text{H I})_{\text{helio}}$ $\text{km s}^{-1}$
(1)	(2)	(3)	(4)	(5)	(6)
NGC 5595	14 24 13.31	−16 43 21.59	237	56	2702
NGC 5597	14 24 27.16	−16 45 46.64	100	36	2698

<sup>a</sup>Position angle of the semimajor axis of redshifted velocities.



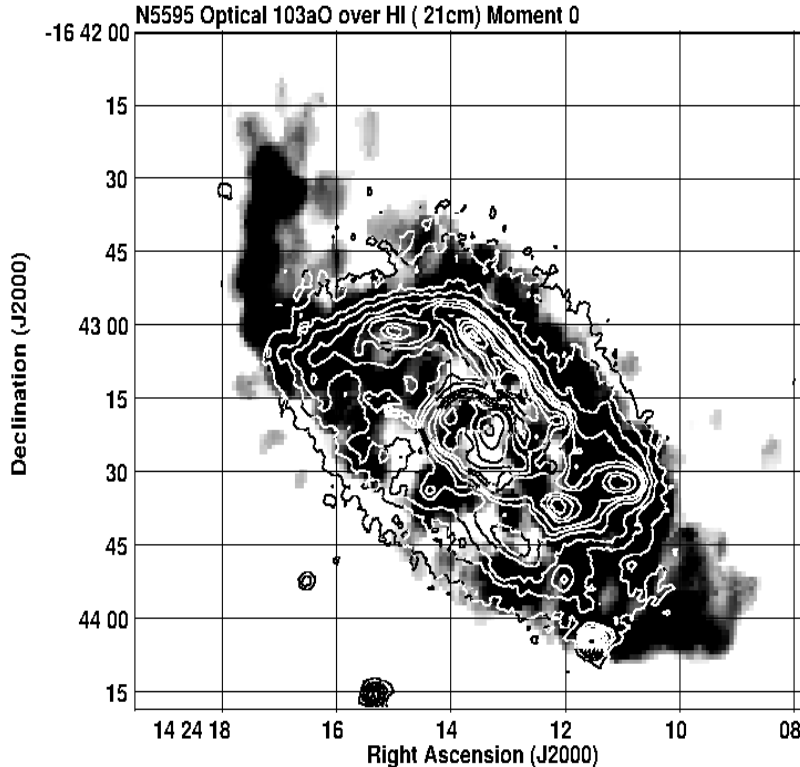


**Figure 12.** Reproduction of the 103aO blue optical emission of NGC 5595 (Diaz-Hernández et al. 2009) in contours superimposed on the H I 21 cm Moment 0 image in grey scale. Optical emission is not flux calibrated; its contours are at 4.7,9,13,20,25,30,40,46,53,60,75 and 92 times  $1\sigma$  where  $1\sigma \sim 90$  in arbitrary units proportional to intensity. The grey scale stretch is from 6.6 to 37 mJy beam $^{-1}$  km s $^{-1}$ . Notice that the H I 21 cm NE and SW elongated structures do not have optical continuum emission counterparts.

The blue continuum image (Figure 1) does not show any extended optical emission or bridges between NGC 5595 and NGC 5597, this fact might indicate that this pair of galaxies are in their early stages of gravitational interaction (Toomre & Toomre 1972; Mihos & Hernquist 1996; Linden & Mihos 2022).

However, our VLA B-configuration observations of both disk galaxies with an angular resolution of  $\sim 7''.14 \times 4''.2$  P.A.  $\sim -11$  deg EofN show that the H I 21 cm emission from NGC 5597 is confined to the extent of its optical disk, while in NGC 5595 the H I 21 cm emission is from its disk, as well as from structures to the NE and the SW that do not have blue optical nor 20 cm continuum counterparts (see Figure 1, Figure 10, and Figure 12).

Computer simulations of gas dynamics and starbursts in disk mergers of similar mass suggest that as the galaxies approach they become severely distorted, forming long tidal tails and a bridge connecting the two disk galaxies (Barnes 1990; Mihos & Hernquist 1994, 1996;

Barnes 1998). A recent retrograde passage dynamical model of the M101 and NGC 5474 reproduces the observations well while suppressing the formation of long tidal tails (Linden & Mihos 2022). The spatial distribution of the cold atomic H I 21 cm gas specially towards the NE and SW outside the optical disk in NGC 5595 suggests that the pair system NGC 5595 – NGC 5597 is in a very early phase of their gravitational interaction with perhaps a retrograde passage (Linden & Mihos 2022).

Table 4 lists the different intrinsic parameters of both galaxies, including the estimated dynamical masses. The angular separation of the galaxies on the plane of the sky is  $3''.97$  and the ratio of their dynamical masses is  $M_{\text{dyn}}^{\text{NGC5595}}/M_{\text{dyn}}^{\text{NGC5597}} \sim 5$ .

From the empirical observational studies of radio continuum emission from pair of disk galaxies, the central sources in barred galaxies are more powerful than in non-barred ones (Hummel et al. 1990). In our study, the barred galaxy NGC 5597 has a nuclear unresolved 20 cm radio continuum source that is about 3.5 times more powerful than the similar source in NGC 5595. Furthermore the innermost central region of NGC 5597

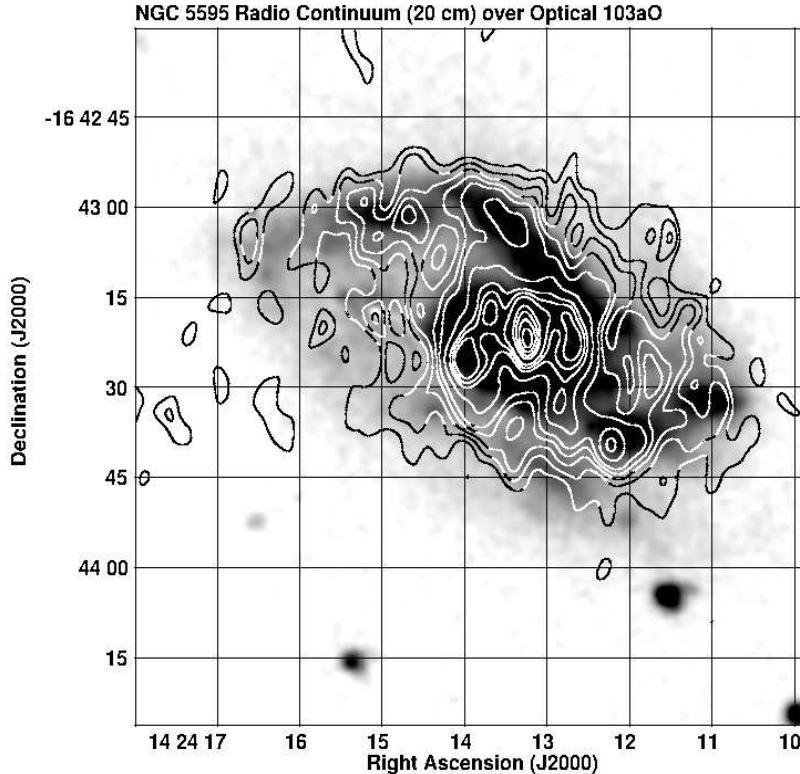


**Figure 13.** Our VLA B-configuration 20 cm radio continuum emission from disk galaxy NGC 5595 in contours superimposed on the reproduction of the 103aO blue optical emission from NGC 5595 (Díaz-Hernández et al. 2009) in grey scale. Contours are at 3, 4, 5, 6, 8, 10, 11, 12, 14, 15, 15.6 times  $1\sigma$  where  $1\sigma \sim 167 \mu\text{Jy beam}^{-1}$ . The brightest 20 cm radio continuum source coincides with the optical nucleus. Two other sources at a distance  $\sim 10''$  from the center toward the east and the west might be part of a circumnuclear structure. There is weak emission from almost all over the optical disk, but no 20 cm radio continuum emission from neither the NE nor the SW H I 21 cm extended structures (see Figure 11).

shows H $\alpha$  and 20 cm radio continuum emissions elongated in the NE - SW orientation (at a P.A. not far from the P.A. of the rotation axis). This innermost region has no H I 21 cm atomic gas emission, while the galaxy shows an H I gas angular velocity curve  $\Omega_{\text{gas}}$  different than the expected  $\Omega_{\text{gas}} \propto R^{-1}$  for a spiral disk galaxy, suggesting an excess of mass. All these observational facts suggest that gas has recently been supplied as fresh fuel into the barred galaxy NGC 5597, while there are H I 21 cm extended structures to the NE and SW in disk galaxy NGC 5595.

We have made a low angular resolution Moment 0 image to search for extended H I 21 cm emission from the field of the pair system NGC 5595 and NGC 5597, using our VLA B-configuration observations, restricting the  $uv$  range from 0 to only  $5k\lambda$  (Figure 14). This resulted in a synthesized beam with FWHM of  $\sim 30''.7 \times 28''.8$  at a P.A.  $\sim +50^\circ$  EofN and  $1\sigma \sim 19.45 \text{ mJy beam}^{-1} \text{ km s}^{-1}$ .

Figure 14 shows no extended intergalactic H I 21 cm emission from any filaments or bridges, but only slightly extended emission from the S and SW and W of NGC 5597 and from NE, SE and SW of NGC 5595<sup>18</sup>.

This negative observational result (no long tidal tails in between NGC 5595 and NGC 5597) is interesting and important because NGC 5597 and NGC 5595 are not only very close on the plane of the sky, but also physically as they both have very similar recession velocities. Table 4 shows the general properties of both NGC 5595 and NGC 5597. These two galaxies also reside in a low galaxy density environment (Tammann 1985; Tully & Fischer 1987). The NGC 5597 - NGC

<sup>18</sup> The lack of extended intergalactic H I 21 cm emission from any filaments or bridges may be due to low surface brightness sensitivity. Future VLA H I 21 cm observations with lower angular resolution, deeper integrating, and therefore better surface brightness sensitivity, would clarify the existence of any intergalactic neutral atomic hydrogen gas in the disk galaxy pair NGC 5595 and NGC 5597.

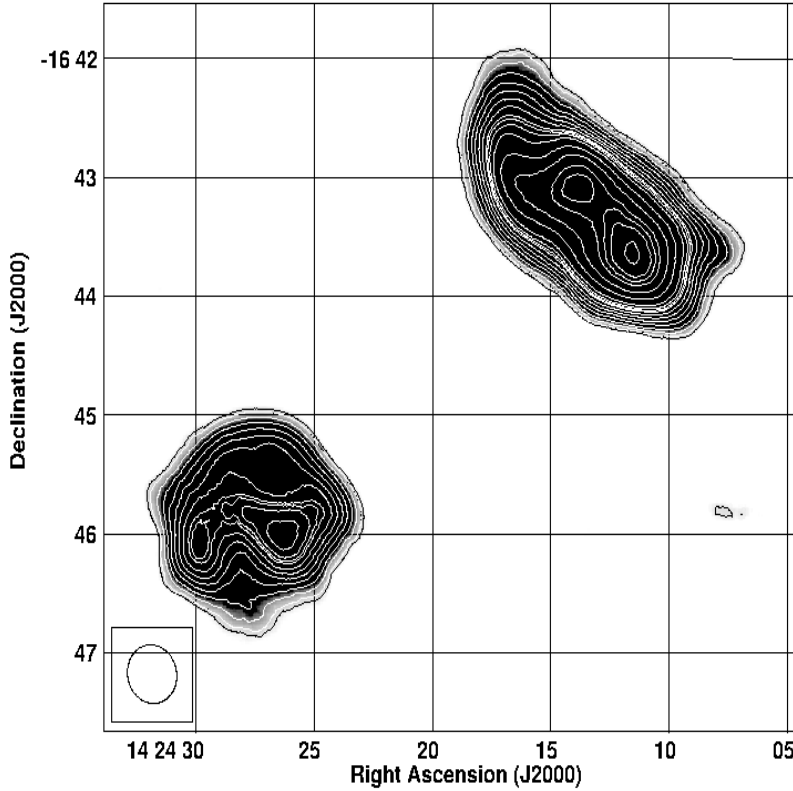


**Figure 14.** Our low resolution VLA B-configuration H I 21 cm Moment 0 image in grey scale and contours, obtained using a  $u, v$  range restricted between 0 and  $5\lambda$ , to search for any H I 21 cm intergalactic extended emission or bridges associated with the disks of NGC 5595 and NGC 5597. NGC 5597 is at south-east, NGC 5595 is at north-west. The grey scale stretch is  $250 \text{ mJy beam}^{-1} \text{ km s}^{-1}$  to  $450 \text{ mJy beam}^{-1} \text{ km s}^{-1}$ . The Moment 0 contours are at 15, 17, 21, 25, 30, 35, 40, 45, 50, 52, 55, 60, 70, 80, 90, 95, 100 and 108 times  $1\sigma$  where  $1\sigma \sim 19.45 \text{ mJy beam}^{-1} \text{ km s}^{-1}$ . No intergalactic H I 21 cm structure or filaments exist between the two galaxies. The synthesized beam at FWHM, which is  $\sim 30''.7 \times 28''.8$  at P.A.  $\sim +50^\circ$  EofN, is shown at the bottom left corner.

5595 system must be in an early stage of gravitational interaction, otherwise if it were in an advance stage the NGC 5595 - NGC 5597 pair system would resemble the antennae or the mice galaxy pairs (Toomre & Toomre 1972; Barnes 1990; Mihos & Hernquist 1996; Barnes 1998; Linden & Mihos 2022). As a comparison, a long tidal H I 21 cm atomic neutral hydrogen gas structure has been detected in the M51 - NGC 5195 system, which are within 5 arcmin on the plane of the sky (Rots, et al. 1990); extended filamentary H I 21 cm atomic neutral hydrogen gas structures have been detected from the M81 - M82 - NGC 3077 system, which are within 80 arcmin on the plane of the sky (Yun, Ho & Lo 1994), and of course the long tidal tails of the antennae system NGC 4038/9 (van der Hulst 1979; Gordon, Koribalski & Jones 2001; Hibbard et al. 2001). Computer N-body simulations have fairly reproduced the stellar and H I (21 cm) long tidal tails of the antennae system (Barnes 1998). However, despite much effort no satisfying model is yet available to repro-

duce the long SE H I 21 cm tidal tail in the M51 system (Toomre 1978; Hernquist 1990; Barnes 1998).

## 7. SUMMARY AND CONCLUSIONS

In this study we have obtained VLA B-configuration H I 21 cm kinematical data from the close pair disk galaxies NGC 5597 SBc(s), and NGC 5595 Sc(s). We have detected for the first time the existence of cold atomic hydrogen H I 21 cm extended structures (streamers) to the north-east, and south-west of NGC 5595 with no blue, nor red optical continuum, nor 20 cm radio continuum counterparts. They may be filamentary features as a result of recent gravitational tidal interaction with its neighbor NGC 5597 to the south-east.

We were able to get the best fit velocity fields, rotation curves ( $V$  vs.  $R$ ), and angular velocities ( $\Omega_{\text{gas}}$  vs.  $R$ ) for both disk galaxies NGC 5595 and NGC 5597 from their heliocentric H I 21 cm recession velocities, assuming gas is in circular orbits around the nucleus. We have presented the H I 21 cm spectra for NGC 5597 and

**Table 4.** Properties of Disk Galaxy Pair NGC 5595 and NGC 5597

Data	NGC 5595	NGC 5597
(1)	(2)	(3)
Optical diameter	$\sim 1'.6$	$\sim 1'.87$
$m_v$	12.6	13.1
$V_{\text{sys}}$	2702 km s $^{-1}$	2698 km s $^{-1}$
$M_{\text{HI}}$	$2.9 \times 10^9 M_{\odot}$	$1 \times 10^9 M_{\odot}$
$M_{\text{dyn}}$	$1.3 \times 10^{11} M_{\odot}$	$2.6 \times 10^{10} M_{\odot}$
$L_{\text{FIR}}^{\text{IRAS}}$	$2.22 \times 10^{10} L_{\odot}$	$2.21 \times 10^{10} L_{\odot}$
P.A. $_{\text{semimajor-axis}}^{\text{red}}$	237° EofN	100° EofN
P.A. $_{\text{rotation-axis}}$	327° EofN	190° EofN
Direction $_{\text{rotation-axis}}$	NW	SW
Peak flux density (20 cm)	2.593 mJy beam $^{-1}$	9.02 mJy beam $^{-1}$
Total flux density (20 cm)	81.83 mJy	36.99 mJy

NGC 5595, estimated the H I 21 cm gas mass from many clouds in both NGC 5595 and NGC 5597, as well as the total H I 21 cm gas mass in both galaxies.

Our H I 21 cm fitted parameters indicate that the disk rotation axis in NGC 5597 projected on the plane of the sky is at P.A.  $\sim 190$  EofN pointing into the SW direction, thus the hemisphere from NW clockwise towards SE is closer to the observer, while the disk rotation axis in NGC 5595 projected on the plane of the sky is at P.A.  $\sim 327$  EofN pointing into the NW direction, thus the NE hemisphere clockwise towards SW is closer to the observer.

We have also presented new 20 cm radio continuum emission images from both NGC 5595 and NGC 5597. In particular in NGC 5597, our image shows an unresolved central emission peak with an elongated structure that coincides with previously published H $\alpha$ +N[II]

line emission. Both emissions come from the innermost central region where there is no cold hydrogen atomic gas in NGC 5597. The existence of H $\alpha$  and 20cm radio continuum, and the lack of H I 21 cm at the center of NGC 5597 are very similar to the distribution observed in other nearby barred galaxies and might suggest a central SMBH with mass of few times  $10^6 M_{\odot}$ .

Finally, we have made low resolution ( $\approx 30''$  at FWHM) H I 21 cm image of the field of the pair disk galaxy system NGC 5595 and NGC 5597 and did not detect any extended intergalactic H I 21 cm tails or bridges in between the disk galaxies.

*Facilities:* EVLA

*Software:* AIPS: (Greisen 2003), CASA (McMullin et al. 2007)

## REFERENCES

- Appleton, P.N., Foster, P.A., & Davies, R.D. 1986, MNRAS, 221, 393
- Argudo-Fernandez, M., Verley, S., Bergond, G., Duarte-Puertas, S., Ramos-Carmona, E., Sabater, J., Fernández-Lorenzo, M., Espada, D., Sulentic, J., Ruiz, J.E. & León S. 2015, A&A, 578, A110
- Athanassoula, E. 1992, MNRAS, 259, 345
- Barnes, J. 1990, *N-Body Studies of Major Mergers in Dynamics and Interactions of Galaxies*, Ed. R. Wielen (Berlin: Springer-Verlag) p. 186
- Barnes, J. 1998, *Dynamics of Galaxy Interactions in Galaxies: Interactions and Induced Star Formation*, SAAS-Fee Advance Course 26, Lecture Notes 1996, Eds. D. Friedli, L. Martinet & D. Pfeniger (Berlin: Springer-Verlag) p. 275
- Binney, J., & Tremaine, S. 1987 *Galactic Dynamics* (Princeton: Princeton Univ. Press)
- Burton, W. B. 1974, *Galactic and Extragalactic Radio Astronomy*, p. 92 (New York: Springer-Verlag)
- Cecil, G. 1988, ApJ, 329, 38

- Combes, F., Boissé, P., Mazure, A., & Blanchard, A. 2002, *Galaxies and Cosmology*, (Springer-Verlag: Berlin)
- Condon, J.J., Helou, G., Sanders, D.B., & Soifer, B.T. 1990, *ApJS*, 73, 359
- Contopoulos, G., 1988, *A&A*, 201, 44
- Contopoulos, G., Gottesman, S.T., Hunter, J.H. Jr., & England, M.N. 1989, *ApJ*, 343, 608
- Cottrell, G.A., 1976, *MNRAS*, 174, 455
- Crane, P., & van der Hulst, J., M., 1992, *AJ*, 103, 1146
- Davies, R.D. 1974 In *The Formation and Dynamics of Galaxies*, IAU Symp. 58, edited by J.R. Shakeshaft (Dordrecht: Reidel), p. 119
- de Vaucouleurs, G., de Vaucouleurs, A., Corwin, H. G., Buta, R., Fouque, R. & Paturel, G. 1993, Third Reference Catalog of Galaxies, RC3 (New York: Springer-Verlag)
- Diaz-Hernández, R., Garcia-Barreto, J.A., & Moreno-Corral, M. A., 2009, *Rev.Mex.Fis.*, E55, 70
- England, M. N. 1989, *ApJ*, 337, 191
- Field, G.F., 1958a, *I.R.E.*, 16, 240
- Field, G.F., 1958b *ApJ*, 129, 536
- Ford, H.C., Crane, P.C., Jacoby, G.H., Lawrie, D.G., & van der Hulst, J.M. 1985, *ApJ*, 293, 132
- Garcia-Barreto, J. A., Carrillo, R., & Vera-Villamizar, N. 2003, *AJ*, 126, 1707
- Garcia-Barreto, J. A., Combes, F., Koribalski, B. & Franco, J. 1999, *ã*, 348, 685
- Garcia-Barreto, J.A., Franco, F., Carrillo, R., Venegas, S. & Escalante-Ramirez, B. 1996, *RMxAA*, 32, 89
- Garcia-Barreto, J. A., Franco, J., & Rudnick, L. 2002, *AJ*, 123, 1913
- Garcia-Barreto, J.A., Mayya, D.Y., & Guichard, J. 2019, *PASP*, 131:094101
- Garcia-Barreto, J.A. & Momjian, E. 2022, *AJ*, 164:91.
- Garcia-Barreto, J.A., & Moreno, E. 2000, *ApJ*, 529, 832
- Garcia-Barreto, J.A., Rudnick, L., Franco, F., & Martos, M. 1998, *AJ*, 116, 111
- Garcia-Barreto, J.A., Scoville, N.Z., Koda, J., & Sheth, K. 2005 *AJ*, 129, 125
- Gebhardt, K., Bender, R., Bower, G. & 12 authors, 2000, *ApJ*, 539, L13
- Geller, M., Kenyon, S. J., Baros, E. J., Jarnett, T.H., & Kewley, L.J. 2006, *AJ*, 132, 2243
- Goad, J. W. 1976, *ApJS*, 32, 89
- Gordon, S., Koribalski, B., & Jones, K. 2001, *MNRAS*, 326, 578
- Greisen, E.W., 2003, *Information Handling in Astronomy - Historical Vistas*, 285, 109
- Haan, S., Schinnerer, E., Mundell, C.G., Garcia-Burillo, S., & Combes, F., 2008, *AJ*, 135, 232
- Haynes, M., Giovanelli, R. & Burkhead, M. S. 1978, *AJ*, 83, 938
- Helou, G., Soifer, B.T. & Rowan-Robinson, M, 1985, *ApJ*, 298, L7
- Hernández-Toledo, H.M., Cano-Diaz, M., Valenzuela, O., Puerari, I., Garcia-Barreto, J.A., Moreno-Diaz, E. & Bravo-Alfaro H. 2011, *AJ*, 142:182
- Hernquist, L. 1990, *Dynamical Status of M51* in *Dynamics and Interaction of Galaxies*, Ed. R. Wielen (Berlin: Springer-Verlag) p. 108
- Hibbard, J. E., van der Hulst, J. M., Barnes, J. E. & Rich, R. M. 2001, *AJ*, 122, 2969
- Ho, L., C., Greene, J. E., Filippenko, A. V. & Sargent, W.L. 2009, *ApJS*, 183, 1
- Ho, L.C. & Ulvestad, J. S., 2001, *ApJS*, 133, 77
- Hummel, E., 1981 *A&A*, 96, 111
- Hummel, E., van der Hulst, J.M., Keel, W.C., & Kennicutt, R. C. Jr., 1987, *A&AS*, 70, 517
- Hummel, E., van der Hulst, J.M., Kennicutt, R. C. Jr., & Keel, W.C. 1990, *A&A*, 236, 333
- Karachentsev, I.D. 1972, *Commn.Special Astrophys. Obs. USSR*, 7, 1
- Karachentsev, I.D. 1981, *Astrophysics*, 17, 135
- Linde, S. T. & Mihos, J. C. 2022, *ApJL*, 933, L33
- Mathewson, D.S., Ford, V. L. & Buchhorn M., 1992, *ApJS*, 81, 413
- McMullin, J.P., Water, B., Schiebel, D., Yound, W. & Golap, K., 2007, in *Astronomical Society of the Pacific Conf. Ser.*, 376, *Astronomical Data Analysis Software and Systems*, XVI, Ed. R.A. Shaw, F. Hill & D. J. Bell, 127
- Merritt, D., & Ferrarese, L. 2001, *ApJ*, 547, 140
- Merritt, D., & Ferrarese, L. 2001, *MNRAS*, 320, L30
- Mihalas, D, & Binney, J., 1981, *Galactic Astronomy*(2nd. Ed. San Francisco: Freeman)
- Mihos, J.C. & Hernquist, L. 1994, *ApJ* 425, L13
- Mihos, J.C., & Hernquist, L., 1996, *ApJ* 464, 641
- Moody, J. W., Roming, P. W. A., Joner, M. D., Hintz, E. G., Geisler, D., Durrell, P. R., Scowen, P. A., & Jee, R. O. 1995, *AJ*, 110, 2088
- Norman, G., & Silk, J., 1983, *ApJ*, 266, 502
- Paturel, G., Thereau, G., Bottinelli, L., Gouguenheim, L., Coudreau-Durand, N. Hallet, N. & Petit, C., 2003, *ã*, 412, 57
- Planesas, P., Scoville, N.Z., & Myers, S.T. 1991, *ApJ*, 369, 364
- Purcell, E. M. & Field, G. B. 1956, *ApJ*, 126, 542
- Reid, M. J., Biretta, J. A., Junor, W., Muxlow, T. W. B., & Spencer, R.E. 1989, *ApJ*, 336, 112
- Rogstad, D.H., Lockhart, I.A., & Wright, M.C.H. 1974, *ApJ*, 193, 309

- Rots, A.H., Bosma, A., van der Hulst, J.M., Athanassoula, E. & Crane, P.C. 1990, *AJ*, 100, 387
- Sancisi, R. 1999, *Galaxy Interactions the HI Signature* in IAU 186 Galaxy Interactions at Low and High Redshifts, Eds. J. E. Barnes & D. B. Sanders (Dordrecht: Kluwer) p. 71
- Sandage, A., & Tammann, G.A., 1981, A Revised Shapley-Ames Catalog of Bright Galaxies (Washington, DC: Carnegie Institution of Washington Publ. 635)
- Scoville, N. Z. 1988, *Galactic and Extragalactic Star Formation* (Dordrecht: Kluwer Academic Publishers NATO ASI Series 232, p. 541)
- Scoville, N. Z., Yun, Mathews, K., Carico, D.P., & Sanders, D.B.. 1988, *ApJ*, 327, L61
- Scoville, N. Z., Yun, M. S., Armus, L., & Ford, H. 1998, *ApJ*, 493, L63
- Spitzer, L. Jr. 1978 *Physical Processes in the Interstellar Medium* (New York: John Wiley & Sons)
- Springob, C. M., Haynes, M. P., Giovanelli, R., & Kent, B. R., 2005, *ApJS*, 160, 149
- Stoche, J. T. 1978, *AJ*, 83, 348
- Stoche, J.T., Tifft, W. G., & Kaftan-Kassim, M.A. 1978, *AJ*, 83, 322
- Tammann, G. A., 1985 ESO Conf. Proc., 20 *The Virgo Cluster of Galaxies*, Eds. O.-G. Richter & B. Binggeli (Garching: ESO)
- Toomre, A. 1978, *Interacting Systems* in IAU 79 *The Large Scale Structure of the Universe* Eds. M. S. Longair & J. Einasto (Dordrecht: Reidel) p. 109
- Toomre, A. 1981, In *Structure and Evolution of Normal Galaxies* edited by S.M. Fall and D. Lynden-Bell (Cambridge University, Cambridge) p. 111
- Toomre, A. 1983, *Theories of Warps in Internal Kinematics and Dynamics of Galaxies* Ed. E. Athanassoula (Dordrecht: Kluwer) p. 177
- Toomre, A. & Toomre, J. 1972, *ApJ*, 178, 623
- Tully, R.B. 1988 *Nearby Galaxies Catalog*, (Cambridge: Cambridge Univ. Press)
- Tully, R.B. & Fischer, J. R. 1987 *Nearby Galaxies Atlas*, (Cambridge: Cambridge Univ. Press)
- Ulvestad, J.S.; Neff, S. G.& Wilson, A. S., 1987, *AJ*, 93, 22
- van der Hulst, J. M., 1979, *A&A*, 75, 97
- van der Hulst, J. M., Hummel, E. & Dickey, J.M. 1982, *ApJ*, 261, L59
- Veilleux, S., Cecil, G., Bland-Hawthorn, J., Tully, R. B., Filippenko, A., V., & Sargent, W. L. W., 1994, *ApJ*, 433, 48
- Wilson, A.S. & Ulvestad, J.S. 1987, *ApJ*, 319, 105
- Woods, D.F. & Geller, M. 2007, *AJ*, 134, 527
- Wright, M.C.H. 1974, Mapping Neutral Hydrogen in External Galaxies in *Galactic and Extragalactic Radio Astronomy* (New York: Springer Verlag)
- Yun, M.S., Ho, P.T.P., & Lo, K.Y., 1993, *ApJ*, 411, L17
- Yun, M.S., Ho, P.T.P., & Lo, K.Y., 1994, *Nature*, 372, 530
- Zwicky, F. 1956, *Ergebnisse der Exakten Naturwissenschaften*, 29, 344